



HHS Public Access

Author manuscript

Drug Discov Today. Author manuscript; available in PMC 2020 February 01.

Published in final edited form as:

Drug Discov Today. 2019 February ; 24(2): 462–491. doi:10.1016/j.drudis.2018.08.009.

Nano-engineered delivery systems for cancer imaging and therapy: Recent advances, future direction and patent evaluation

Ghazal Nabil^{1,2}, Ketki Bhise¹, Samaresh Sau¹, Mohamed Atef², Hossny A. El-Banna², Arun K. Iyer^{1,3}

¹Use-inspired Biomaterials & Integrated Nano Delivery (U-BiND) Systems Laboratory, Department of Pharmaceutical Sciences, Eugene Applebaum College of Pharmacy and Health Sciences, Wayne State University, Detroit, MI, USA

²Department of Pharmacology, Faculty of Veterinary Medicine, Cairo University, Giza, Egypt

³Molecular Imaging Program, Karmanos Cancer Institute, Wayne State University School of Medicine, Detroit, MI, USA

Abstract

Cancer is the second highest cause of death worldwide. Several therapeutic approaches, such as conventional chemotherapy, antibodies and small molecule inhibitors and nanotherapeutics have been employed in battling cancer. Amongst them, nanotheranostics is an example of successful personalized medicine bearing dual role of early diagnosis and therapy to cancer patients. In this review, we have focused on various types of theranostic polymer and metal nanoparticles for their role in cancer therapy and imaging concerning their limitation, future application such as dendritic cell cancer vaccination, gene delivery, T-cell activation and immune modulation. Also, some of the recorded patent applications and clinical trials have been illustrated. The impact of the biological microenvironment on the biodistribution and accumulation of nanoparticles have been discussed.

Introduction

Use of nanotechnology for health care has been evolving for many decades, and several innovative drug delivery system such as Doxil™ and Abraxane™ demonstrated their clinical relevance by increasing drug efficacy, targeting ability and decreasing toxicity [1]. The possibility of therapeutic achievement associated with nanoparticles (NPs) is dependent mainly on their ultra-small size, tumor tissue selectivity and being harmless to coexisting healthy tissue while presenting improvement in their toxicity profile [2]. Besides this, the therapeutic NPs could be simultaneously used for molecular imaging for disease diagnosis [3]. Theranostics is a modern terminology derived from two words *therapeutics* and *diagnostics* [4]. Theranostics is an emerging aspect of personalized medicine composed of

Corresponding authors: Iyer, A.K. (arun.iyer@wayne.edu).

Author contributions

GN and KB are responsible for the manuscript write-up, Dr. HEB provided the design, and Dr. AKI provided overall direction for the review as well as critical evaluation of the manuscript.

Conflicts of interest

The authors declare no conflict of interest.

both therapeutic agent and diagnostic agent in one formula guided by a targeting ligand directed to the malfunctioned cells as shown in Fig. 1 a & b [5]. The concept of this combination is that both medical and diagnostic agents need to be sufficiently accumulated in the affected tissue to give the desired effect [6]. There are unique opportunities to use multifunctional formulations for both diagnostic and therapeutic purposes [7–12]. It was reported that metal, lipid, polymer nanoparticles have a wide range of biomedical properties that can be exploited for theranostic applications [13–15]. Moreover, they can be encapsulated with cytotoxic drugs, such as paclitaxel, doxorubicin (DOX), gemcitabine, and other such drugs and labeled with antibodies for active delivery purposes [16–18]. Theranostic nanoparticles have multi-tasking ability such as controlling tumor growth, invasion and metastasis of cancer [19,20] in addition to their imaging property. The critical difference between the conventional diagnostic tools and the theranostics agents is that the latter one allows imaging before, during and after drug administration [6]. That will help the physician not only to diagnose and target the cancer tissue but also to monitor the drug distribution, accumulation, release and to determine if the patient is a responder or non-responder to this therapy as shown in Fig. 2 [21]. This is possible by their versatile characteristics that aim to provide “the right patient with the right drug at the right dose that has been achieved by early diagnosis.” Theranostic NPs can be engineered for selective delivery of the cytotoxic payload to the cancerous cells by manipulating size, composition, and targeting ligand, in addition to their ability to accumulate in leaky tumor vasculature via Enhanced Permeability and Retention (EPR) effect. Additionally, theranostic nanoparticles are engineered with anti-fouling polyethylene glycol (PEG) and zwitterionic agents to delay renal filtration, thus endowing them with prolonged plasma circulation and overcoming nonspecific liver and spleen uptake. NPs are a flexible matrix which able to combine different substances in one system such as lipid, polymer, and metal also; they could be combined with different imaging probes such as radioactive substances, fluorescent probes, and quantum dots to serve the theranostic purpose. Radical alteration on the metabolic cell signaling pathways is considered a milestone feature for cancer existence. Discovery of these altered pathways underlies the development of molecular targeted anticancer agents [22]. Identification of various tumor biomarkers was impactful on the level of screening, diagnosis, prognosis, and development of targeted therapy [23]. Theranostic nanoparticles can be employed in the active targeting of the tumor cell or its subcellular components by the aid of these biomarkers. Theranostic NPs could be administrated with different routes such as intravenous [24,25], intraperitoneal [26], transdermal[27], subcutaneous [28], orally [29] and pulmonary route [30]. This review focuses on the inherent feasibility of various types of theranostic polymer and metal NPs and their applications in cancer diagnosis and treatment. The impact of the tumor microenvironment on the bio-distribution and accumulation of NPs with the recent attempts to overcome the biological barriers has been broadly discussed. Moreover, the limitations and future applications in cancer vaccination, T-cell modulation, and gene therapy have been illustrated.

Theranostic nanoparticles are all in one system composed of tumor targeting ligand, tumor imaging agent and tumor therapeutic agent. These nanoparticles are enabled to accumulate in tumor tissue by both EPR-effect [31,32] and⁴ receptor-mediated endocytosis. EPR effect is a cancer characteristic phenomenon which paves the way for tumor passive targeting. EPR

comes from the leaky tumor vascular endothelium concomitant with improper lymphatic drainage. Unlike the healthy blood vessel, the tumor endothelium is fenestrated which enables nanoparticles localization by extravasation. The drug concentration will increase by several folds due to improper lymphatic drainage [33]. Receptor-mediated endocytosis is a new approach for cancer active targeting. Active targeting is the ability to direct the drug-loaded system to the desired site by surface functionalization with ligands which will be selectively recognized by receptors on the surface of particular cells. As an example of active targeted therapy; DOX PEGylated liposome decorated with anti-HER2 affibody (Table 1) was used to target HER2 overexpressing breast cancer. The results showed selective HER2+ tumor cytotoxicity concomitant with increased DOX concentration when compared to HER2-tumor [34]. Both passive and active targeting are utilized to increase the concentration of therapeutic NPs in the tumor side and to decrease the systemic toxicity.

The flexibility of theranostic NPs enables the usage of different types of the therapeutic agents such as chemotherapeutic agents, gene therapy, photothermal therapy and photodynamic therapy with various types of imaging agents such as fluorescent dyes, fluorescent polymers, quantum dots, metal nanoparticles, and magnetic nanoparticles. The efficiency of theranostic NPs can be improved by enhancing their stability and targeting ability. Stability of the NPs can be enhanced by surface modification with stealth agents such as Poly (ethylene glycol) (PEG) which will improve stability and evade recognition and immature localization in the reticuloendothelial system (RES). Active targeting with different molecules such as antibodies, affibodies, and specific ligands will improve the accumulation of theranostic NPs in the tumor side.

Impact of the tumor microenvironment on the biodistribution and accumulation of nanoparticles

The recent development of the engineered nanoparticles have the potential to revolutionize the diagnosis and treatment of cancer; for example, active targeting of the NPs to a specific subcellular compartment within the cancerous cell. While EPR permits the extravasation and accumulation of NPs, the opsonization, trapping by RES, high interstitial pressure (IFP), dense stroma, blood–brain barrier (BBB) and stratum corneum (SC) limit the homogenous and adequate intra-tumoral distribution of NPs. Nevertheless, the advances in understanding the impact of NPs features such as size, shape and surface properties on the biological interactions are promising for the effective consequential development of NPs capable of overcoming the biological barriers. As well as the tumor microenvironment can be employed to serve the biomedical application of the NPs as discussed in this section. Here is addressed some of the biological cofactors versus some of the biological barriers.

Biological cofactors

Enhanced Permeability and Retention (EPR) effect—Matsumura and Maeda first identified the impact of this phenomenon on the biodistribution and accumulation of the NPs in the tumor side [36]. EPR defined as an imbalance between the blood supply and the

⁴<https://www.worldscientific.com/worldscibooks/10.1142/p429>.

lymphatic drainage of the solid tumors. As the cancerous tissue overgrows, the need for nutrient and oxygen supply is increased resulting in the formation of neovasculature in a process known by angiogenesis [37]. The healthy capillaries characterized by intact endothelial cell lining surrounded by pericyte and sealed externally by a basement membrane and controlled by a layer of smooth muscle. Unlike the healthy vasculature, the tumor neovasculature characterized by porous endothelial lining [38] (0.1–3 μm in diameter) [37] with diminished pericyte layer and basement membrane in addition to the absence of muscular control [39–41]. Moreover, the improper lymphatic drainage leads to an improper drain of the tumor mass. Leaky tumor vasculature causes extravasation of NPs while impairment of lymphatic drainage causes accumulation of nanoparticle [36]. However, EPR is employed in NPs delivery to the solid tumor with a reduction of the systemic toxicity; the therapeutic level is not sufficient. It was reported that the concentration of the NPs in the solid tumor with the aid of EPR is only two folds over other organs which is not sufficient to induce a potent therapeutic effect [42]. To overcome the insufficient NPs accumulation in the cancer tissue many strategies have been developed such as surface functionalization with active targeting molecules, modifying NPs surface hydrophilicity and charge, adjust the NPs size and control tumor blood flow. Amongst the active targeting modalities is the affibody. Affibody is a small molecular weight protein (around 6.5 kDa) with high binding affinity to a given targeted structure. It gets considerable attention in the theranostic biomedical research due to their unique features. Here is a simple comparison between antibody and affibody as a targeting ligand in Table 1 [43].

Smart-responsive nanoparticles—The tumor microenvironment with its unique features such as acidic pH, hypoxia, active efflux pumps, hyperthermia, upregulated oncogenic proteins and altered redox potential play a vital role in the destabilization of chemotherapeutic agents, reducing anticancer drug concentration in the tumor side and developing of chemotherapeutic resistance. These challenges motivated the development of many approaches such as (1) development of tumor-activated pro-drug therapy (2) external stimuli-responsive NPs therapy, (3) intratumoral stimuli-responsive NPs therapy, and (4) active targeted NPs. The tumor-activated prodrug therapy based on the administration of the drug on its inactive form and upon reaching to the tumor side, the tumor microenvironment will facilitate its conversion to the active form. This strategy will help in reducing the systemic toxicity of the cytotoxic drugs, increasing the half-life time with reducing the dose frequency of unstable medications, increase the drug potency by increasing the concentration of active form in cancerous tissue only [48]. As an example of prodrug therapy, modification of the drug structure to have a high binding affinity to plasma protein which will increase the half-life time of the drug and decrease its renal elimination. Developing of a water-soluble maleimide derivative of doxorubicin with a MMP-2 specific peptide sequence showed high binding affinity to plasma albumin. The free doxorubicin will be liberated from the doxorubicin albumin-bound form by matrix metalloproteinase-2 (*MMP-2*) which is highly expressed in some tumors. The doxorubicin prodrug was more potent than the free doxorubicin when tested in melanoma xenograft model which characterized by the presence of high level of MMP-2 [49]. External stimuli-responsive NPs or remotely triggered NPs or smart system is defined as remotely controlling the release of the drug from its cargo by externally controlled stimulus. This system is superior to the

conventional systems and will provide unique, promising clinical benefits. Remotely triggering of NPs could be achieved by photodynamic therapy (PDT), photothermal therapy (PTT), ultrasound, electro-thermal, magneto-thermal, X-ray, radiofrequency, and laser. This system is able to localize the NPs in the appropriate tumor location; as an example, magnetic NPs can be directed to the tumor tissue by creating a magnetic field in the tumor area. This for sure will prevent inappropriate drug dissemination and subsequent systemic toxicity. Also, this system provides the capability of burst release (one-time use) or pulsatile release (on-demand release); as an example, the laser beam leads to irrevocable changes in the carrier will be used for one-shot payload release, or if it led to reversible changes in the carrier, it would be used for pulsatile payload release. Turning “on” or “off” possibility will provide control over the location, timing, dose concentration and the undesired drug metabolism will be prevented by the stimuli-responsive carrier which will only release the drug on the desired site based on controlled external stimuli. ThermoDox is an example of remotely triggered NPs which is on phase III clinical trials. ThermoDox is a heat-activated liposome encapsulating doxorubicin. Increasing the temperature by radiofrequency or ultrasound will lead to structural changes of the liposome wall with subsequent release of doxorubicin [50]. Intratumoral stimuli-responsive NPs therapy is defined as the usage of the unique features of the tumor microenvironment such as acidic pH, overproduced enzyme, and hypoxia to liberate the drug from its carrier. The tumor-responsive NPs is significantly utilized to reduce the systemic toxicity, overcome chemotherapeutic resistance, and to control tumor growth. Here is an example of acidic pH-responsive liposome for the delivery of paclitaxel and Bcl-2 siRNA in melanoma cell lines and xenograft model. The nanocarrier composed of kojic acid backbone-based cationic amphiphile incorporating endosomal pH-sensitive imidazole ring. The synergistic combination in this formulation was able to counteract the drug resistance by knocking down the Bcl-2 and sensitize the tumor to the chemotherapeutic effect of paclitaxel. The animal studies showed carrier compatibility with significant tumor regression owed to the synergistic combination [51]. The acidic pH of the tumor environment was smartly utilized in the fluorescent switch for precise cancer diagnosis. Recent study synthesized pH-responsive fluorescent graphene quantum dots (pRF-GQDs). This pRF-GQDs display a sharp fluorescence transition between blue and green at switching point pH 6.8. The particles are blue at the normal physiological pH, but it switches to green on the tumor acidic pH. The color switching property of this particles will be helpful in distinguishing between the cancerous and normal tissue [52]. He group just develops another example for fluorescent switchable theranostic NPs. They make use of the elevated glutathione and ATP level in the tumor environment to develop redox/ATP switchable theranostic NPs which used as a tool to monitor the release of doxorubicin. The NP consists of a fluorescent probe (FAM) and a quencher (BHQ-1) conjugated to an adenosine-5'-triphosphate (ATP) aptamer and its complementary DNA (cDNA), respectively. Later, doxorubicin was incorporated in the DNA duplex to form (FBA@-DOX). The FBA@DOX was mixed with glutathione-responsive polymer poly(ethylene glycol)-*block*-poly (aspartic acid-*graft*-cystamine) (PAS). This NP was turned “off” on the regular glutathione and/or ATP level, but it is turned “on” the tumor milieu characterized by an elevated level of glutathione and intracellular ATP. Once the polymer is stimulated and the DNA degraded, the doxorubicin is released, and the fluorescent is recovered to monitor doxorubicin release [53]. Active targeting is defined as decorating the surface of NPs with a

targeting molecule which is able to direct the NPs to the tumor side. Currently targeting tumor hypoxia has gained considerable attention especially in treating solid tumors. A recent study developed hypoxia-targeting NPs consist of human serum albumin (HSA) as a carrier decorated with acetazolamide (ATZ) to deliver paclitaxel to triple negative breast cancer cell lines. ATZ is the ligand for carbonic anhydrase IX (CA IX) receptor which is overexpressed in tumor hypoxic condition. The results showed that the hypoxia-targeted formulation is more potent than the free paclitaxel and non-targeted formulation. The ligand was able to deliver the paclitaxel payload to CA IX expressing breast cancer [54]. This four different approaches can be applied individually or together and can be used for delivering therapeutic agent alone or imaging agent alone or to be used as a theranostic tool.

Biological barriers

Opsonization, phagocytosis, and reticuloendothelial system (RES)—

Opsonization is the process of coating the foreign antigen with opsonin proteins to be more attractable to phagocytic cells. Opsonization or fouling is carried out by nonspecific adsorption of plasma proteins such as albumin, fibrinogen, and apolipoproteins on the antigen surface. Mononuclear phagocytic cells distributed in the lung, liver, and spleen are part of the immune system known by the reticuloendothelial system (RES), and they are highly attracted to opsonized molecules [55]. The hydrophobicity, the size and the charge of the NPs will determine if they are going to be opsonized or not [56]. It was found that the hydrophobic negatively charged particles with large size are rapidly trapped in RES [57]. Many strategies have been addressed to overcome RES trapping such as increasing the hydrophilicity and neutralize the NPs charge by stealth or antifouling agents such as dextrans and polyethylene glycols (PEGs). Also, reduction of the NPs size below 35 nm was found to be helpful in evading the RES [55]. By passing RES trapping of NPs will increase their circulating time, maintaining their therapeutic concentration which will reflect on their pharmacodynamic profile. Doxil, the first FDA approved PEGylated NPs which showed improved stability [58].

Interstitial fluid pressure (IFP)—The IFP in the cancer tissue is higher than healthy tissue by 10–40 folds [59]. Both IFP and acidic pH are limiting factors for the NPs. The IFP difference between the tumor center and surrounding healthy border lead to interference with NPs diffusion [60]. IFP originated from the imbalance between the tumor blood supply and lymphatic drainage with increased tumor mass and increased the extracellular matrix component (ECM) [61]. Acidic pH is mainly because cancerous cells tend to use anaerobic glycolysis for energy production which leads to overproduction of lactic acid. Over accumulation of the produced lactic acid is increased due to lack of lymphatic drainage leads to decreasing the pH. This acidic pH leads to destabilizing of anticancer agent and suppresses the immune system. The new approach is to develop tumor microenvironment-responsive nanoparticles.

Extracellular matrix (ECM)—Stromal matrix plays a vital role in maintaining homeostasis, supporting cells, storage of cellular regulatory substances, adjusting the organ physical properties and allowing the cell to cell communication. The ECM is composed of stromal cells, ECM component, and ECM associated component. Stromal cells such as

fibroblasts, pericytes, endothelial cells, and immune cells. The ECM component is produced locally by the tissue fibroblast such as osteoblast and chondroblast. Two major macromolecules are generated to form the ECM, glycosaminoglycans (GAGs) polysaccharides and fibrous proteins. GAGs such as hyaluronan, chondroitin sulfate, dermatan sulfate, heparan sulfate, and keratan sulfate which are covalently bound to fibrous proteins such as collagen, elastin, fibronectin, and laminin to form proteoglycans. While the ECM-associated component such as enzymes and growth factors which are responsible for regulation of cell functional and proliferative activity [62]. Modified ECM is a hallmark in cancer development and is responsible for cancer metastasis, elevation of IFP and drug resistance. Cancer-associated fibroblasts (CAFs) are the key player in tumor modified ECM [37]. Tissue fibroblasts are transformed to CAFs under the influence of tumor-associated growth factors such as transforming growth factor beta (TGF- β), stroma-derived factor (SDF-1), platelet-derived growth factor (PDGF), and basic fibroblast growth factor (bFGF). CAFs are responsible for overproduction of ECM and hence tumor fibrosis. Also, they are responsible for induction of ECM remodeling via matrix metalloproteinase (MMP). Stroma transformation playing a crucial role in pancreatic ductal adenocarcinoma (PADC) development, metastasis, and drug resistance. Many pharmacological strategies have been developed to overcome the ECM barrier and improve nano-sized drug delivery such as induction of ECM shrinkage by injection of a hypertonic solution, hyperthermia, radiofrequency (RF) or high-intensity focused ultrasound (HIFU).

Blood–brain barrier (BBB)—Central nervous system (CNS) microenvironment is one of the most challengeable microenvironments of the body due to the presence of blood–brain barrier (BBB). BBB is a cellular protective barrier which prevents the passage of harmful substances to the CNS and regulates its homeostasis. It is composed of tight, impermeable endothelial lining covered with a layer of astrocytes. BBB permits selective transport of essential molecules to the brain and precludes the passage of other substances through the tight endothelial junction and efflux pumps. BBB is considered one of the limiting factors for brain tumors and neurological disorders therapies because it hampers their delivery to CNS [63]. In this respect, several strategies are carried out to improve the delivery of therapeutic NPs across the BBB to CNS such as active targeting of NPs to transferrin. Transferrin is only expressed in brain endothelial lining. Anti-transferrin targeted immunoliposome revealed increase uptake *in vitro* and *in vivo* [63].

Stratum corneum (SC)—Stratum corneum is known to be the primary barrier of the skin. SC is the external thin layer overlying skin epidermis. The SC composed of 15–20 layers of dead cells called corneocytes. Corneocytes characterized by the absence of the nuclei and cellular organelles and packing of keratin protein embedded in filaggrin matrix. The corneocytes are encased in a cornified envelope and surrounded by an extracellular lipid layer. The function of SC is to prevent body dehydration and protect against infection and mechanical stress [64,65]. Transdermal drug delivery (TDD) gained considerable attention as an attractive alternative for oral and injection routes due to skin large surface area, non-invasive, painless, overcome needle phobia, bypass stomach degradation and pre-systemic liver metabolism which will improve bioavailability, as well as, avoid systemic toxicity, suitability for unconscious and vomiting cases, and not expensive. Moreover, The TDD is a

peerless route for protein and peptide vaccination due to over-accumulation of dendritic cells in the dermal and epidermal layer which play a vital role in antigen presentation and evoking of the immune response [66]. Although the TDD has unique features, it faces many challenges to be used for local and systemic therapeutic administration due to SC. The lipid milieu of SC delivers only lipophilic, and small molecular weight (<500 Da) drugs but not hydrophilic and macromolecules, and it is used as a reservoir for many therapeutic agents such as corticosteroids and contraceptive to provide sustained release and limit administration frequency [67]. TDD is widely used topically for skin disorders, in contrast, the usage of TDD for systemic therapy is growing slowly as since the first FDA approved scopolamine for motion sickness in 1979 till now around twenty medications have been FDA approved for systemic application. This limited number of systemically approved TDD drugs will increase continuously due to the discovery of many techniques that will overcome the SC barrier [68]. These techniques are divided into chemical, biochemical and physical approach which aimed to increase the penetration of the applied drug through SC. The chemical approach includes off-the-shelf compounds such as ethanol and methanol, customized compounds such as Azone (1-dodecylazacycloheptan-2-one) and synthesis of prodrug by adding a cleavable chemical group or cleavable enzymatic linker for example; linking of cyclosporine with a polyarginine-heptamer cell-penetrating peptide. The biochemical approach includes phage display, polyarginine, and natural pore-forming peptide magainin. The physical approach includes stripping, iontophoresis, electroporation, ultrasound, thermal ablation, laser, microdermabrasion, microneedles, radio-frequency [68]. Nanotechnology is emerging as an unprecedented tool for enhancing TDD. One of the transdermally applied NPs applications is for skin cancer. Although skin cancer is not the most fatal form of cancer, it is the most common malignancy in the USA. However, Melanoma incidence is very low, but it is responsible for the majority of skin cancer deaths. Surgical excision is the gold standard for the localized lesions, and it is accompanied by high survival rates. NPs are effective in the treatment of metastatic melanoma which is fatal for 80% of the patients. Here is one study used curcumin loaded liposome as anti-melanoma by TDD. Liposome prepared from soybean phospholipids showed significant anti-melanoma activity *in vitro* and *in vivo* when compared to free curcumin. Liposome enhances the potency of curcumin in TDD [27]. Hung group found that 1,2-dipalmitoyl-snglycero-3-phosphocholine (DPPC) liposome increase the topical efficacy of 5-aminolevulinic acid (5-ALA) by increasing its penetration through skin SC. 5-ALA is a drug used for the treatment of skin cancer with photodynamic therapy (PDT). Sufficient penetration of 5-ALA to SC is one of the limiting factors because 5-ALA is hydrophilic. They found that the 5-ALA loaded liposome was potent in decreasing melanoma cell viability and in increasing intracellular reactive oxygen species (ROS) when compared to free drug. In melanoma xenograft model the liposome showed better penetration to skin with selective accumulation in tumor side. They suggest that the liposome would be a promising nano-carrier for 5-ALA in TDD mediated PDT [69]. In general, nanocarriers seem to be a promising approach in TDD because they decrease skin irritation, increase the protection of encapsulated drug, enhance the penetration of loaded drug and suitable for topical combination therapy [70].

Application of theranostic nanoparticles on cancer cell lines

Theranostic polymer nanoparticles

Polymer-based NPs are a broad class with unique attractable features and behaviors which potentiate their application in different fields. Polymers are large molecular weight substances [71] which can be classified to natural and synthetic or degradable and non-degradable. Natural, biodegradable polymer includes polysaccharides such as (chitosan, sodium alginate and dextran) and proteins such as (gelatin, and albumin). Natural polymers are natural abundance, water-soluble, nontoxic, non-immunogenic, biocompatible, biodegradable, stable, easily manipulated, not costly [72], abundant surface functional groups which could be utilized for ligand tagging and surfactant coating for enhanced delivery with high drugs binding affinity and smoothly cellular uptake [73]. One of the FDA approved natural polymer composed of albumin-bound paclitaxel (nabTM-paclitaxel; Abraxane®); which was approved in 2005 for the treatment of metastatic breast cancer. The natural polymers lack batch-to-batch uniformity, formulation amenability, and manufacture associated problems [74,75]. Synthetic polymers are classified to biodegradable such as poly (lactic acid) (PLA), poly(glycolic acid) (PGA) and their copolymers, poly (lactide-coglycolide) (PLGA) which is FDA approved [75,76] and nonbiodegradable such as polystyrene (PS) [77]. The synthetic biodegradable polymers could be tailored for specific biomedical application by controlling their porosity, degradation time and their physicochemical properties. Also, they have batch-to-batch uniformity, long shelf time, reproducible and cheaper than the biological polymers. Moreover, they could be produced on a large scale [78]. Polymers can be classified based on their structure to solid polymer NP, polymer micelle, polymer conjugate, dendrimer, a polymersome, polyplex, emulsion droplet, nanocapsule, nanosphere, hydrogel and polymer-lipid hybrid system [79–82] as shown in Fig. 3a & b. Polymers are used as vehicles for the delivery of various therapeutic agents such as drug, protein, combined therapy [83] ribonucleic acid (RNA) [84] and imaging agent [85]. Using polymer-nanoparticle significantly impacts the pharmacokinetic and pharmacodynamics of the loaded drug [86] due to their biodegradability, biocompatibility, non-toxicity, and nonimmunogenicity [87]. Moreover their application in the formation of stealth NPs which plays a vital role in prolonging the drug circulation time and reduce RES trapping. Also, the choice of polymer and the method of preparation can be used to modify drug release which makes them ideal candidates for controlled release therapy for cancer, vaccines, and contraceptives. Also, they can be utilized for active and passive drug delivery to cancer. In tumor passive targeting the NPs accumulated by EPR [88] while active targeting or transcytosis or receptor-mediated endocytosis could be achieved with surface functionalization with antibodies, affibodies, and ligands which will be only recognized by particular cells. Many receptors were found to be overexpressed in various cancer such as folate receptor, epidermal growth factor receptor (EGFR), human epidermal growth factor receptor 2 (HER2) and glucose-regulated protein of 78 kDa (GRP78) [89] which can be employed in active tumor targeting. The ability to deliver the polymer NPs to the specific site will reduce their systemic toxicity profile and increase their potency [90]. Many polymer NPs formulations have found their way to the market such as PEGASYS® (an example for polymer–protein conjugate containing PEGylated interferon alfa-2a for hepatitis C infection), Doxil® (an example of stealth liposome containing DOX for cancer)

and Genexol-PM® (as an example for block copolymer micelle containing paclitaxel for cancer).

One of the utmost usages of NPs is the **polymer–lipid hybrid** system which combines the advantages of both liposome and polymer NPs. Here is one study used core–shell lipid-polymer NPs for co-delivery of two therapeutic agents in addition to imaging agent for castration-resistant prostate cancer. Prostate cancer is considered the second leading cause of death in men. The first therapeutic agent is docetaxel which is the first line of treatment of metastatic prostate cancer. Docetaxel has the common toxic symptoms of the most chemotherapeutic agents such as fatigue, hair loss, GIT disturbance in addition to febrile neutropenia. The second therapeutic agent is the sphingosine kinase 1 (SK1) inhibitor FTY720 (fingolimod) as SK1 is a proto-oncogene which is highly expressed in prostate cancer and responsible for chemotherapeutic resistance. The main obstacle which hinders the extended application of FTY720 is its induction of lymphopenia. In this study, they supposed that FTY720 would increase the sensitization of the prostate tumor to docetaxel. The used imaging agent was rhodamine B *in vitro* and CF488 *in vivo*. The carrier core composed of poly-(D,L-lactide-*co*-glycolide) (PLGA) which act as a scaffold for docetaxel while the shell consisting of a mixture of phospholipids and cholesterol and act as a matrix for FTY720 and CF488. Using of FTY720 as a tumor sensitizer has reduced the effective dose of docetaxel four folds. The formulation was high serum stability, long shelf life and the carrier was biocompatible. The *in vitro* results showed time-dependent cellular uptake, sustained intracellular release with an enhanced release on acidic pH when tested on androgen resistant cell lines PC-3 and DU145. Animal xenograft model results showed that the formulation was as effective as the free combination but without the toxic symptoms associated with the free combination such as 20% loss of body weight, liver shrinkage, and lymphopenia. The fluorescent CF488 label showed more than 40% accumulation of the formulation in the tumor side. That means that the formulation has the same efficacy of free therapies but with outperform toxicity profile [94].

In this regard, **polymer-polymer conjugates** have a promising fingerprint in cancer research. In a representative study, two types of polymer NPs were tested against human cervical carcinoma. The first NP consists of a triblock copolymer poly (ethylene glycol)-b-poly (glutamic acid)-b-poly (ethylene glycol) (*GEG*). The second NP consists of a diblock copolymer poly (ethylene glycol)-b-poly (glutamic acid) (*EG*) conjugated with folic acid for active targeting to form (EGFA). Methotrexate (MTX) was encapsulated in each formulation to form M-GEG and M-EGFA NPs. Both polymers showed cytocompatibility and hemocompatibility proved by *in vitro* sulforhodamine B protein-dye assay (SRB). Immediate cellular uptake was determined by fluorescence-activated cell sorting (FACS) in human cervical carcinoma (HeLa). Significant apoptosis was detected by acridine orange (AO), and ethidium bromide (EB) staining. For pharmacokinetic and bio-distribution studies ^{99m}Tc (Technetium) radiolabeled M-GEG and M-EGFA NPs were intravenously injected into HeLa xenografted athymic mice models. The whole body scanning with Gamma-Single-Photon Emission Computed Tomography (SPECT) showed passive and active accumulation of both MTX loaded NPs. Increasing the survival rates of the treated mice indicate the potent anticancer effect of these polymer NPs. This study proved the availability

to use these NPs as a potential theranostic replacement for both chemotherapeutic and diagnostic agent for cervical carcinoma [96].

Fluorescent dyes are not far away from theranostic applications for cancer diagnosis and therapy. Fluorescent molecules, fluorophores or fluors distinctly light up in the presence of light. Each fluorophore has its characteristic features which potentiate its usage in a given biomedical application. Fluorescent agents are basically used to tag specific cellular organelles with high specificity for precise evaluation. Fluorescent molecules are classified into intrinsic and extrinsic fluorophores. Intrinsic or natural or auto-fluorescence or biological fluors are natural proteins present in the cell and have the fluorescent criteria enable them to be used as a fluorescent tag for bioimaging purpose. They are permanent and have self-generation property. They can be used for monitoring gene activity and tagging of specific protein or organelles or the entire cell which could be tracked in tissue. They could be divided to non-photoactivable; form chromophore in the presence of oxygen and photoactivable; form chromophore in the presence of light. Natural fluors used for biomedical applications are present with different colors such as green fluorescent protein (GFP) (bright green), TagBFP (blue), mCitrine/mVenus (green–yellow), mCherry and mApple (red), tdTomato (orange), mCerulean3 (cyan), and mKate2 and mNeptune (far-red). GFP, the first and the most common natural fluor is small and chemically inert. It emits a bright green light upon exposure to UV or blue light, and it is widely used for monitoring gene activity and transfection efficiency. The other natural fluors emit red color provide better cell penetration, reduced autofluorescence in red emission range which enables them to be used for monitoring tumor progression in mice. Although the natural fluors have a wide range of biomedical applications, they have some limiting issues. GFP is not stable during fixation and subsequent processes, their expression in mice are breed variable, its aggregation is cellular toxic, prolonged light excitation produces free radicals, and it is not suitable for establishing GFP expressing cell lines because it induces apoptosis. mEosFP is other natural fluor which is unstable at 37.8 °C, so it is not applicable to mammalian cells and only limited to plant, insect and zebrafish. DsRed fluorescent protein is toxic to the hematopoietic system which limits its application in tracking the hemopoietic cells. Tagging of certain protein with fluorescent protein should not impair its structure, function, cellular localization but it was noted in some cases that protein tagging impairs its cellular function and localization. Moreover, fluorescent proteins have limited physicochemical properties, not very bright, not photo-stable, intermittently blinking in addition to that; their application is time-consuming [97]. Extrinsic fluorescent agents can be classified to organic dyes and quantum dots. Fluorescence organic dyes used in cell biology are broadly classified as under [98]:

1. Cell and tissue staining dyes such as Rhodamine B, FITC, TRITC, Alexa Fluor® dyes.
2. Nucleic acids and proteins labeling dyes such as Cyanines: Cy2, Cy3, Cy5, Cy7.
3. DNA staining dyes include DAPI, Hoechst family, Propidium Iodide, Acridine Orange.
4. Compartment and organelle-specific dyes include, but are not limited to MitoTracker® (mitochondria), LysoTracker (lysosome), FM 4–64® and FM 5–

95@ (vacuole), DiOC6 (endoplasmic reticulum), BODIPY (lipid and membrane labeling), NBD C6-ceramide (Golgi apparatus).

Fluorescein was the first fluorescent organic dye used for biomedical application followed by synthesis of many derivatives of the original compounds. These organic dye derivatives are with greater performance over the biological or natural fluors due to their solubility, photostability, distinct excitation/emission spectra, sensitivity, optimal quantum yields and excitation coefficients. Their small size favors their application in bioconjugation with macromolecules such as antibodies, biotin, and avidin without interfering with their biological functions. Their high stock shift (the difference between absorption and emission maxima) gives them high photostability and bright imaging property with low background. Their photostability enabled their application in long-term imaging to investigate the biological process, pathological conditions and therapeutic potency. Molecular engineering and nanotechnology have emerged as a promising tool to improve the photostability of the organic dyes. One of the recently published molecularly engineered fluors is the fluorescent dye, 2,5-bis(6-amine-benzoxazol-2-yl)thiophene (BBTA) which showed high photostability, high stock shift, no noise and low cytotoxicity in addition to its simple preparation by a two-step reaction [99]. Fluorescent organic dyes have been extensively used for studying the biodistribution and target-ability of the NPs as clarified by many examples also, they have been clinically validated.

Quantum dots are more brighter and more photostable with high fluorescent intensity than organic dyes. Quantum dots (QDs) are a tiny nanocrystal with 2–10 nm diameters. The QDs composed of core, shell and polymer coat. The core of QDs consists of semiconductor materials such as cadmium selenide (CdSe), cadmium telluride (CdTe), indium phosphide (InP), and indium arsenide (InAs) while the shell consists of aqueous organic coat such as ZnS. The core of the QDs determines the color of the emitted fluorescence while the shell is responsible for improving their optical properties and enhancing their photostability by preventing quenching of emissive core excitons. Polymer coat is accountable for enhancing QDs solubility, but it also could increase their size than GFP and organic dyes which will limit their cellular uptake; they will be internalized to the cell either by targeting ligand or phagocytosis. Their optical properties are affected by their shape and size; the small size emits colors with a short wavelength such as blue and green while the big size QDs emits colors with a long wavelength such as red and orange. Their name is coming from confining electrons in a limited space due to their small size. They display a unique electronic properties intermediate between their bulk and atomic semiconductors. Due to their narrow emission, prolonged lifetime, pure bright fluorescence and broad UV excitation; QDs have been adopted for a lot of biomedical application. Among them, theranostic NPs with QDs has received considerable attention due to the ability to use them for bioimaging, real-time monitoring, combination with various types of NPs such as polymer or metal NPs and the availability of surface functionalized with certain targeting molecule for drug delivery purpose [100] QDs are known to be the best for monitoring siRNA delivery. Targeting ligand is very important to avoid nonspecific binding and undesired distribution of QDs which will lead to misinterpretation. The toxicity of the QDs depends on variable factors such as size, shape, concentration, solubility, composition, charge, surface coating, redox activity and exposure time. The toxicity of QDs is mainly associated with heavy metal core and

production of free radicals during their excitation. Controlling the length of exposure and concentration will be helpful in toxicity reduction [97].

Apart from these, there are some drugs which can also be used as biocompatible fluorophores because of their inherent, intrinsic fluorescence characteristic. Examples of this class include doxorubicin, curcumin [101,102].

Many examples for combining the polymer NPs with fluors are explained in this section. One example of actively targeted **polymer** nanoparticle was tailored to target (HER2) overexpressing ovarian cancer cell line. The polymer used in this study was poly (allylamine) hydrochloride reacted with sodium phosphate in the presence of polyethylene glycol (PEG) as a surface modifier. The core of NPs was loaded with indocyanine green (ICG) near-infrared dye (NIR) while the surface was decorated with anti- HER2 monoclonal antibody. The ability of this theranostic nanosystem to combine both fluorescent imaging and photothermal therapy was tested by continuous exposure to 808 nm NIR laser irradiation in two different ovarian cell lines with a variable HER2 expression SKOV3 and OVCAR3. The results showed an increase in the cellular uptake and efficacy of photothermal therapy of the anti-HER2 targeted formulation than both non-targeted and free ICG in HER2 overexpressing SKOV3 cell line [103]. PLGA (poly (D,L-lactide-co-glycolide)) is a versatile polymer used in various drug delivery applications. It is biocompatible and can encapsulate external drug payload at a good loading efficacy. Rhodamine B, a cell-staining fluorescent dye, was used as a representative molecule for loading in polymer mixture and demonstrated uptake of the polymer micro-/nanoparticles in A549 human lung cancer cell line [104]. Another natural thermo-responsive biodegradable polymer NPs; chitosan-*g*-poly (*N*-vinylcaprolactam) was used to load curcumin. The result showed higher fluorescence intensity on the uptake in PC3 prostate cancer cells than normal L929 cell line. This system was more cytotoxic and more apoptotic in cancer cell line versus normal cell lines [101]. Novel pH-responsive polymeric micelles based on polyethylene glycol (PEG) and cholesterol were synthesized for delivery of water-insoluble anticancer drug camptothecin (CPT). This polymer was biocompatible and nontoxic. The release of the micelles payload was based on the acidic pH. *In vitro* cytotoxicity of micelles proved the chemotherapeutic potency this nanosystem. Intracellular localization was studied by encapsulating of coumarin 153 dye and visualizing by confocal microscopy. The model cell lines used were MCF-7 and HeLa [105]. Poly(L-lactide)-*b*-polyethylene glycol (PLA-*b*-PEG) polymer NPs was used for sequential delivery of combinatory chemotherapy to triple negative breast cancer. The delivered chemotherapeutic agents were erlotinib and doxorubicin. This nanocarrier promoted burst release of erlotinib with pulsatile release of Dox; this release mode showed enhanced cytotoxicity. Tumor accumulation of this system was validated by encapsulation of the Cy5.5 dye which was injected into syngeneic orthotopic breast tumor model via tail vein of mice. The nanoparticles were localized at the tumor site via the EPR effect and showed strong near-infrared fluorescence [106]. Wang *et al.* have studied the useful application **nanomicelles** as a theranostic tool in triple negative breast cancer. Hyaluronic acid targeted and non-targeted nanomicelles were prepared from Styrene Maleic Anhydride (SMA), and FDA approved vitamin E TPGS to from (HA-SMA-TPGS) and (SMA-TPGS) respectively. The nanocarrier was loaded with curcumin analog

(CDF) and tested on MDA-MB-231 and MDA-MB-468 triple-negative cell lines. The targeted formulation was more potent and more apoptotic followed by nontarget then free CDF. The *in vitro* cell uptake and *in vivo* tumor accumulation of targeted and non-targeted nanomicelles was carried out by encapsulating with rhodamine B and S0456 near-infrared dye respectively. The targeted formulation showed higher cell uptake and high tumor accumulation [107].

Polymersomes are widening the perspective to be one of the most popular theranostic NPs. It is considered as a polymer vesicle consisting of variable amphiphilic block copolymers to give the final core-shell structure at which there is availability to encapsulate the hydrophilic drug in the core and incorporate the hydrophobic drug on the shell. Polymersomes can have a modified architecture to fit unprecedented controlled release of drugs, functionalization with targeting ligands, allowing biodegradability and compatibility and combining both contrast and therapeutic agents to form theranostic NPs [108]. Doxil® is one of many liposome-based products used for the treatment of various types of cancer. Liposome has attracted attention for therapeutic applications because it consists of natural biocompatible self-assembled phospholipid and it provides the ability to encapsulate both hydrophilic and hydrophobic drugs. However, many factors have been merged to limit its application such as physical and chemical stability and chemical versatility. Polymersome outperforms its counterpart well-established liposome due to its physical and chemical stability and chemical versatility. Polymersome combines the advantages of liposome and polymer assemblies as it can encapsulate both hydrophilic and hydrophobic drugs as liposome but with a significant decrease in critical aggregation concentration (CAC) over lipids and with 500 times higher membrane shear viscosity over lipid membrane as illustrated in Fig. 4 [109]. An attempt to direct the polymersome to precise subcellular localization was carried out by Mallik group. In this study, they focused on mitochondrial-targeted fluorescent polymersome loaded with DOX for drug delivery to pancreatic cancer. Mitochondrial was targeted due to its vital role in cancer progression, metastasis, and development of multiple drug resistance. DOX selection based on its ability to affect mitochondrial membrane integrity and mitochondrial DNA synthesis besides its ability to inhibit topoisomerase II. For this purpose amphiphilic polymer poly(lactic acid)-*co*-poly(ethylene glycol) (PLA-PEG) was used as a polymer-some building block, and fluorescent analog of triphenylphosphonium cation (TPP) was used as an imaging agent and targeting ligand. TPP is able to transfer the drug-loaded system through the inner mitochondrial membrane. NPs characterization showed polymersome with 89 ± 6 nm size and 9 ± 0.8 mV zeta potential. The polymersome bilayer structure was confirmed by confocal microscopy with the aid of FM1-43 dye. Subcellular localization was observed by overlapping of red MitoView stained mitochondrial and green fluorescent polymersome in BxPC-3 pancreatic cells. DOX-loaded targeted polymersome significantly decrease BxPC-3 cellular viability when compared with free DOX and non-targeted formulation [110]. Glioma is the brain and spinal cord glial cells cancer. Glioma characterized by a poor prognosis and limited life expectancy due to the existence of BBB and multidrug resistance (MDR). A lot of studies to address these hindrances are going on, one of these studies used smart polymersome to target glioma. The features of this polymersome make it smart are as following: application of synergistic combination therapy by encapsulating of both DOX, as an anticancer agent, and tetrandrine

(Tet), as a multidrug resistance inhibitor. Surface functionalization with lactoferrin as a targeting ligand, lactoferrin was proved to be more efficient than transferrin as a brain targeting ligand, in addition to that lactoferrin is overexpressed in both BBB and glioma cells so that it will enhance both bypassing BBB and accumulating drug in glioma cancer cells. Moreover, the polymersome was prepared from biodegradable polymer methoxy poly(ethylene glycol)-poly(ϵ -caprolactone) (MPEG3k-PCL15k) and α -carboxyl poly(ethylene glycol)-poly(ϵ -caprolactone) (HOOC-PEG3.4k-PCL15k). *In vitro* cytotoxicity and cell uptake studies showed significant enhancement of the targeted polymersome with combination therapy over the other groups. The 1,1'-Dioctadecyl-3,3',3'-tetramethylindotricarbocyanine Iodide (DiR), a near-infrared dye was used for tracking the formulation in glioma model rat. *In vivo* Imaging of DiR-Loaded Polymersomes showed significant homing of the targeted polymersome 3.6 time higher than the non-targeted formulation. Targeted formulation with combination therapy shows significant inhibition of glioma with better life expectancy [111]. Lactoferrin targeted polymersome paves the way for it is feasibility as chemotherapeutic and/or imaging vehicle for glioma model. Another study was carried out to get the benefit from the tumor microenvironment by developing hypoxia-responsive polymersome. The overgrowth of the solid tumor mass with lack of sufficient oxygen supply leads to the development of hypoxic tumor environment. Hypoxia is one of the characteristic features of the solid tumors as breast, prostate, colon, and pancreatic cancer. Hypoxia is involved in many cancer pathways such as cancer metastasis, angiogenesis, remodeling of ECM, and multiple drug resistance. The hypoxia-responsive polymersome composed of diblock copolymer PLA-azobenzene-PEG was used to encapsulate gemcitabine and erlotinib for the treatment of pancreatic cancer. The sensitivity polymersome to the hypoxic condition was tested by encapsulating carboxyfluorescein dye in the polymersome. The polymersome encapsulating carboxyfluorescein dye was used to treat BxPC-3 cells grown under normoxic condition and hypoxic condition (1% oxygen level). The fluorescent imaging showed that under hypoxic condition 90% of the encapsulated dye was released within 50 min with no significant release under normoxic. BxPC-3 cells were cultivated in three-dimensional spheroids agar (to mimic the hypoxic condition) and treated with polymersome encapsulating gemcitabine and erlotinib. The results showed a significant decrease in the cell viability with hypoxia-responsive polymersome when compared to free drugs and formulation used under normoxic condition. These results pave the way for the promising application of hypoxia-responsive polymersome in the theranostic field [112].

Polymer micelles also have a broad application in the field of oncology [113]. Polymer micelles can be combined with quantum dots for theranostic applications. Here is a study which combines the therapeutic effect of DOX and the imaging property of the cadmium selenide (CdSe) quantum dots in one phospholipid based polymeric nano-micelles carrier. The construct composed of 1,2-distearoyl-sn-glycero-3-phosphoethanolamine-*N*-[methoxy (polyethylene glycol)-2000] (DSPE-mPEG-2000), 1,2-distearoylglycero-3-phosphocholine (DSPC) and prepared by lipid hydration method. DOX and CdSe were loaded into the hydrophobic core of the micelles. Transmission electron microscopy (TEM) and Dynamic light scattering (DLS) showed nano-micelles with approximately 50 nm. The nano-micelles characterized by seven days sustained release leading to a constant pool of drug available for

the cells for longer time when compared with free drug. Cell uptake was found to be time-dependent with a confocal microscope. The potency of DOX and compatibility of CdSe in the nano-micelles was determined by *in vitro* viability assay in HeLa cell line which showed the compatibility of CdSe and the potency of the nano-formulation over the free DOX [114].

Polymeric dendrimer such as poly (amidoamine) (PAMAM) was used to improve the systemic viral gene delivery therapy. A comparative study was carried out to figure out the optimum delivery condition for theranostic sodium iodide symporter (NIS) gene. NIS gene is one of the oldest well-known theranostic agents in thyroid cancer. It has the capability to aggregate iodine in the thyroid gland which used for its imaging and radiotherapy. Ability to transduce cancer cells with NIS gene will be helpful in cancer monitoring and pave the way for the application of radioiodine therapy. For this study, three groups were tested in the hepatic cancer-bearing mouse. The first group was only plain adenovirus with NIS gene, while the second group was the adenovirus with NIS gene coated with PAMAM dendrimer and the third group was typical to the second group in addition to anti-(EGFR) decorating ligand GE11. *In vitro* testing showed enhanced cellular uptake in receptor-mediated formulation than the non-targeted formulation. *In vivo* results showed specific tumor accumulation and increased anticancer activity of targeted formulation followed by non-targeted coated formulation when compared to nonspecific liver accumulation gained by plain control formulation as shown in Fig. 5. To confirm the efficacy of anti-EGFR active targeting, another study was carried by injecting cetuximab anti-EGFR monoclonal antibody before systemic injection of the GE11 targeted coated formulation. Moreover, a combination of radio-viral therapy was screened by a therapeutic dose of ^{131}I after the different formulation. The results revealed promising output for the combined therapy with a broad safety margin [115].

Polymer dependent stealth nanoparticle is one of the useful applications of polymer in nano-therapy. One study demonstrated the useful usage of ^{111}In -DTPA-labeled pegylated liposomes (IDLPL) in a patient with several cancer subtypes. On the studies performed on a patient with mucocutaneous AIDS-related Kaposi sarcoma (stage T₁I₁S₁) the gamma camera scanning of whole patient's body which lasts for 7 days revealed localization of the formulation in the tumor-related regions such as a left limb, upper right arm, and forehead as shown in Fig. 6. Continuous research efforts to develop surface-modified liposomes are straight-forward progressing. The incorporation of MPEG (PEGylating) into liposomal membrane leads to increase its circulating time. In addition to enhancing steric stability against plasma protein and cell receptors which are responsible for immature capturing, immobilization and destabilization, evading the reticuloendothelial system (RES) sweeping after intravenous administration of traditional liposome. Moreover, the pharmacokinetics and toxicity profile for the encapsulated agent is improved [116]. Biopolymer not only used to configure liposome but also superparamagnetic iron oxide. One of this application composed of superparamagnetic iron oxide nanoparticles (SPIONs) core surrounded by a biopolymer shell. The biopolymer shell consists of polyethylene glycol (PEG), polyethyleneimine (PEI) and polysorbate80 (Ps 80) at which DOX was incorporated to form DOX-Ps 80-SPIONs. Characterization of this system revealed 58 nm particle size, 28 mV zeta potential, 29.3 drug loading and 24.1 emu g⁻¹ magnetization saturation. The *in vitro* cytotoxic study showed

increased cell penetration of the former composite when compared to control free DOX. In glioma animal model superparamagnetic iron oxide had a dual role, the first was as magnetic resonance imaging (MRI) contrasting agent and the second as a magnetic targeting agent. This nano-platform showed improvement in glioma curing after 28 days due to increasing formulation deposition in cancer tissue by two factors, application of magnetic field and by Ps80-induced endocytosis. The same result was confirmed by *ex vivo* studies such as Prussian blue dye and fluorescent doxorubicin assay (Fig. 7). The formulation was safe and compatible with various organ, especially cardiac tissue. The oncolytic effect of the formulation depends on induction of caspase 3 apoptotic axis [117].

Theranostic metal nanoparticles

Apart from theranostic polymer nanoparticles, another important class of theranostics, metal and metal oxide nanoparticles, has garnered considerable attention. Continuous improvements to achieve maximum therapeutic benefits out of metal and metal oxide nanoparticles present promise to the future of nanomedicine. These efforts aim to improve the delivery of the drug by combining physical aspects like heat, light, ultrasound with the primitive drug delivery system. Both iron oxide and gold nanoparticles have forayed their way to approval by food and drug administration (FDA) [14]. Gold and iron nanoparticles have excellent contrast imaging property, which is exploited to achieve a diagnosis of tumors. The toxicity of silver nanoparticles limits their application. Furthermore, chemotherapeutic agents can either be covalently attached to the surface of nanoparticles or can be encapsulated into secondary delivery vehicles like liposomes or polymer micelles [118]. Apart from these, few other metal nanoparticles such as barium, bismuth, calcium, magnesium, nickel, titanium are being investigated for their theranostic applications [119]. As the current cancer therapy is moving towards immune-checkpoint antibody inhibitors, the use of theranostic nanoparticles, encapsulated with programmed death-1 (PD-1) siRNA and tumor macrophage inhibitors have become a viable strategy for adjusting tumor-infiltrating immune cells [120]. Moreover, surface functionalization of the NPs with ligands that are selectively recognized by receptors on the surface of particular cells will increase their transcytosis uptake.

Great interest toward the formation of **magnetic nanoparticle** (MNPs) for nanomedicine application is due to their ability to localize the drugs in affected tissue using magnetic fields, in addition to the ability to use them as a contrasting agent for MRI. Moreover, MNPs can be utilized for the induction of apoptosis via magnetic hyperthermia. The terms iron oxide nanoparticles and superparamagnetic iron oxide nanoparticles (SPIONs) shall be used interchangeably in the context of this review. As an example, the versatile ligand hyaluronic acid (HA) that targets CD44 overexpressing breast cancer cells was conjugated on the external surface of superparamagnetic iron oxide nanoparticles (SPIONs), and the nanoparticle was coupled with photothermal therapy, where it showed the rapid generation of heat on NIR irradiation [121]. PAMAM dendrimer conjugated onto the surface of SPIONs presents dual purpose: encapsulation of 3,4-difluorobenzylidene-curcumin (CDF) anticancer drug within the intricate dendrimer architecture, facilitating its sustained release, and SPIONs core that serves as an excellent MRI contrast. This hybrid system has improved tumor targeting ability using folate targeting to folate-receptor overexpressing ovarian cells

SKOV3 and cervical HeLa cells [3]. In another study, DOX was loaded onto SPIONs coated with PEG, and PEI polymer. At which surface functionalization with folic acid aimed to increase NPs internalization by endocytosis. The size of DOX-FA-SPIONs was 67 nm, with improved release of DOX in tumor acidic pH. Surface functionalization showed enhanced accumulation of the NPs in both MCF 7 cells *in vitro* and in mice bearing MCF 7 xenograft which was monitored by confocal laser scanning microscope (CLSM) and MRI, respectively. DOX-FASPIONs coupled with magnetic field showed significant tumor suppression *in vitro* and *in vivo*. Formulation safety was confirmed by the absence of any toxicological signs in liver, lung, kidney, and heart after chronic administration [122]. Pancreatic cancer is known to be challenging due to the impermeability of the stroma. Stroma is not only responsible for tumor proliferation and metastasis, but also responsible for the development of drug tolerance which leads to poor prognosis and increased mortality rate [123]. Stromal targeting is a promising strategy in the treatment of the tumor with dense stroma such as pancreatic cancer. For instance, iron oxide nanoparticle (IONPs) loaded with gemcitabine, a chemotherapeutic agent and decorated with urokinase plasminogen activator (uPA), targeting agent was used. uPA targets stromal cells, cancer cells and tumor-associated cells overexpressing urokinase plasminogen activator receptor (uPAR). It was found that uPAR is overexpressed in around 86% of pancreatic cancer tissues including tumor cells, tumor endothelial lining, tumor-associated fibroblasts, and macrophages. Serine protease uPA is involved in many tumor-associated metabolic pathways such as cancer metastasis, matrix degradation, and angiogenesis. These theranostic nanoparticles deliver both IONPs contrasting agent and gemcitabine chemotherapeutic agent to pancreatic cancer. This formulation is considered smart stimuli-responsive NPs as the release of gemcitabine is pH and lysosomal enzyme dependent. The basic construct of this formulation consists of three axes: the first is the formation of the polymeric coated magnetic iron oxide NPs, the second is the linking of chemotherapeutic gemcitabine, the third is the conjugation of uPA ligand. The polymer-coated IONPs was synthesized with 22 nm size. Then gemcitabine was linked to the polymeric coat of IONPs by lysosomally cleavable tetrapeptide linker Gly-Phe-Leu-Gly (GFLG). The uPA ligand was conjugated to the IONPs via its amino-terminal fragment (ATF). The uPA is responsible for receptor-mediated endocytosis of the whole formulation while the GFLG is responsible for the intracellular release of the gemcitabine. GFLG is cleavable by lysosomal cystein protease and cathepsin B which are extensively produced in pancreatic cancer. The ATF-IONPs-GEM revealed a reduction of systemic toxicity, improve of the MRI due to increase accumulation of IONPs in the tumor side, prolonged effect of gemcitabine due to the protection of the payload from nonspecific degradation and prevention of premature drug release. All of these factors were contributed to significant growth inhibition of pancreatic cancer in xenografted mice [124]. While lipid nanoparticles do not pose problems with systemic incompatibility and have sustainable manufacturing techniques [125], their use is limited in theranostic context. However, they can be repurposed by coupling with metal nanoparticles with the aim to achieve maximum benefit out of both these systems. SPIONs conjugated with a NIR dye and further coated with a lipid bilayer targeting hepatocellular carcinoma via the galactosamine targeting ligand were developed with exhaustive characterization [126]. While aggregation can be a major limitation with SPIONs, our experience says that coating with various agents can ameliorate the condition. Here is the first pioneer study combined polymerosome with magnetic

nanoparticles (MNPs) to form magnetopolymerosomes. In which well-tailored polymer vesicle was stuffed with MNPs. In these composite MNPs could be used as a contrasting agent for MRI, formulation director via magnetic field and induction of magnetic hyperthermia. Magnetic hyperthermia is applied to trigger drug release and induce cells death. Also, the core of polymer vesicle is suitable for loading of the therapeutic agent. The magnetopolymerosomes is a flexible theranostic tool [127].

Gadolinium has also found its way to theranostic oncology field. Several chemotherapeutic combination studies have been used for cancer treatment [128]. Similarly, many therapeutic and diagnostic agents have been combined in the same nanoparticle platform for cancer diagnosis and treatment. One vehicle consisted of poly-(D,L-lactide-co-glycolide) (PLGA) has been used for delivering boron-curcumin complex (RbCur) and gadolinium into ovarian cancer (IGROV-1) cells. The Surface of the vehicle was functionalized with folate to enhance formulation transcytosis. In this formulation, boron and gadolinium were used for neutron capture therapy (NCT) simultaneously with the anti-cancer effect of curcumin. Gadolinium had a dual role in this formulation: The first was in NCT and the second as an MRI contrasting agent. The findings from this study indicated that folate enhanced formulation internalization and the combination of NCT and curcumin enhanced ovarian cancer cytotoxicity [129]. The pH-responsive doxorubicin-loaded pegylated gadolinium oxide NPs (Gd-PEG-dox NPs) were used for synchronized therapeutic and imaging purpose. Dox fluorescence revealed high cellular uptake after incubation for 3 h. Gadolinium would be used as a contrasting agent for MR imaging. The cytotoxicity of the synthesized NPs was confirmed on A-549, PANC-1 and U-87 cancerous cell lines which represent lung, pancreatic, and brain cancer respectively [130].

Manganese ion (Mn^{2+}) plays an undeniable role as a contrasting agent. Characteristic theranostic redox-sensitive nanoscale coordination polymer (NCPs) is an example for Mn^{2+} diagnostic application. It is known that glutathione (GSH) is overproduced in many types of cancer and it is combined with chemotherapeutic resistance to DOX, platinum drugs, alkylating agents and arsenic [131]. In the current study manganese ion (Mn^{2+}) was reacted with dithiodiglycolic acid disulfide linker (SS) to form mesoporous Mn-SS NCPs. At which DOX was loaded to form Mn-SS/DOX NPs. These Mn-SS/DOX NPs were coated with polydopamine (PDA) and (PEG). The disulfide linker is cleavable in the presence of an elevated level of GSH in cancerous cells with subsequent release of DOX. The formulation is more cytotoxic than free DOX in different cell lines. Also, it showed efficient tumor homing with efficient tumor regression when compared to free DOX *in vivo*. This formulation could be utilized for theranostic application due to the presence of Mn^{2+} , MRI contrasting agent [132].

Gold has a glory of reputation in the theranostic nanoparticles applications as regarding stability; gold nanoparticles are excellent because they do not aggregate to the extent of SPIONs. Even their MRI contrast is not as sharp as iron oxide nanoparticles, but this does not deter their launch in the market after stringent FDA approval. The versatility of gold nanoparticles is evident from the various modules they are coupled with to achieve a theranostic response. Positron emission tomography (PET), SPECT, MRI, X-ray based computed tomography (CT) are some of the common imaging modalities explored to a wide

extent for gold nanoparticles. Gold was combined with quantum dots and silica as a multi-component optical nanosystem in glioma cell lines. In this nanosystem, gold can be utilized as a mediator for photothermal therapy or bioimaging purpose [133]. Gold can be applied to cancer gene therapy, gold nanoparticles with dexamethasone surface-modification showed selective uptake in cancer cells over-expressing glucocorticoid receptors. Study aims to modulate glucocorticoid responsive element (GRE) gene to induce an antitumor effect by down-regulating p-AKT [14]. Like SPIONs, gold nanoparticles can also be surface-decorated with dendrimers and used for dual imaging purpose [134]. Gold nanoparticles have been reported as efficient probes for diagnosis of leukemia by some research groups [135] and for early diagnosis of human squamous cell carcinoma (SCC) by Rachela Popovtzer group. PEGylated gold nanoparticles with 30 nm size were prepared and divided into two groups: one with anti-EGFR monoclonal antibody as an active tumor targeting ligand and the other one with anti-rabbit immunoglobulin G (IgG) antibody as a passive negative control. Mice with anatomically non-detectable SCC were intravenously injected with targeted and non-targeted formulation with continuous screening with CT. The results showed a significant difference between targeted and non-targeted formulation at 6-h time point at which the actively targeted formulation reached its maximum plateau while the passive targeted withdrew gradually from the tumor. Also, the CT value of the targeted formulation was 190 ± 12 HU when compared to 34 ± 5 HU of non-injected mice as shown in Fig. 8. These findings prove by definitive evidence that the tumor biomarker is more precise and predictive in cancer diagnosis rather than anatomical growth. This study showed the ability to use gold nanoparticles as a non-invasive tool for early diagnosis of cancer [136]. Curcumin is a natural compound with a high potential for therapeutic applications which is limited by its poor solubility and bioavailability. Nanosystem composed of water-soluble hyaluronic acid-curcumin (HA-Cur) conjugated to gold NPs (AuNPs) by chloroauric acid reduction method to form (HA-Cur @AuNPs). The surface of the formed (HA-Cur@AuNPs) was subsequently functionalized by folic acid conjugated polyethylene glycol (PEG-FA) to form (PF-HA-Cur@AuNPs). This nanosystem showed haemocompatibility which enabled its intravenous administration. Also, the cytotoxicity of this system was more potent than free Cur when tested on HeLa, C6 glioma, and Caco-2 cell lines which represent cervical, brain and colorectal adenocarcinoma cancer. Many studies were done to check the cellular uptake and intracellular localization of this system. Confocal microscopy showed high cellular uptake of FITC-labeled PF-HA-Cur@AuNPs in glioma and Caco-2 cell lines while the fluorescent microscopy revealed nuclear and perinuclear accumulation of rhodamine B isothiocyanate-labeled PF-HA-Cur@AuNPs on HeLa cell lines with Hoechst 33342 nuclear staining [137].

Silver nanoparticles have an established record in the infectious disease domain; although their recent entry in cancer therapy is yet to have a strong foothold [138]. In the current study, silver nanoparticles coated with chitosan and bearing an interesting triangular shape have been engineered to operate in the NIR photothermal therapy against non-small cell lung cancer [139]. Silver NPs have been successfully prepared with different shapes such as nanorod, nanodisk, nanoprism, nanowire, nanosphere, nanoflower, etc. [140] to be utilized for shape-dependent optical and electronic property studies. Among them, triangular nanoprism silver NPs has gained considerable attention due to its interesting optical

properties [141]. Triangular silver NPs has high localized surface plasmon resonance (LSPR) when compared with spherical silver NPs [142] which potentiate their applications, not only as biosensors but also as plasmonic enhancers and as conductive inks [143]. Also, silver NPs are prone to oxidation in the presence of chloride ions so that many studies provide a protective coating from gold [143] or chitosan to them. Silver NPs prepared by biosynthetic reduction method showed antibacterial, anti-malignancy to different cell lines and compatibility to various cells. This NPs can also be utilized for diagnostic approach because it elicits red fluorescent color [144]. Silver nanocluster (Ag NC) was coupled with paracetamol prodrug and functionalized with folic acid as a targeted ligand. The non-toxic prodrug paracetamol is activated to a toxic compound by the high level of ROS in the cancer cell. The induction of apoptosis in this study was promoted by Ag NC and activated paracetamol. Ag NC was utilized for imaging the localization of the entire formulation [145]. As it is known that the physicochemical properties such as color, fluorescent intensity, and absorption features of metals particles are size dependent. The silver nanocluster is smaller than silver NPs with complete different optical properties [146]. Silver NC is brighter in color (bright yellow) with bright intense fluorescence [147], photostable with low toxicity [148]. Many types of nanoparticles have shown stimuli-dependent activation. This stimulus could be externally induced such as light and magnetic field or internally present under certain disease conditions such as pH and enzymes [149].

Zinc oxide nanoparticles have received extensive attention in recent years as a metal oxide theranostic NPs due to their large surface area, excellent electromagnetic character, ability to dissolve in both acidic and basic environment, and feasibility of surface modifications due to increased OH group density on its surface. Hong and his group synthesized red fluorescent zinc oxide NPs that were conjugated with TRC105 targeting ligand to breast cancer vascular endothelial and conjugated with ^{64}Cu radioisotopes for PET imaging. These NPs are suitable for cancer fluorescent and PET imaging [150]. Zinc nanowires are also under active research for their optical imaging properties [151].

Future prospects of theranostic nanoparticles

Cancer vaccination

One of the promising applications of theranostic nanoparticles is their application in dendritic cell cancer vaccination. Theranostic is an urgent requirement in this selective type of immunization due to the need to check two vital processes: the first is the antigen loading to dendritic cells and the second is the migration of the antigen-loaded dendritic cells to the nearest lymph node to present the loaded antigen and stimulate the immune system against malignancy. Both of these checkpoints will determine the efficacy of vaccination and the recovery percent. Cancer vaccination depends on triggering the immune system against cancerous cells bearing tumor-associated antigens (TAAs) on its surface. TAAs are not entirely different from normal cellular proteins. The TAAs could be a particular tumor antigen, restricted neonatal protein abnormally produced in adult or could be aberrantly produced normal protein either in amount or structure. These abnormal proteins are immunogenic and trigger the immune system for example; the anti-p53 antibodies which were detected in patients with metastatic breast cancer which indicate abnormal production

of p53 in these cases [152]. Sometimes the immune system is not stimulated against these abnormal proteins due to many factors such as; cancer patients are immuno-compromised, these proteins are closely related to normal proteins, the ability of cancer cells to suppress the immune system and initiate immune tolerance state. These concepts were turned upside down after the discovery of (1) Tumor-specific antigen. (2) Co-stimulatory factors such as **Granulocyte Macrophage Colony Stimulating Factor (GM-CSF)** that is able to potentiate T-cells response and overcome immune tolerance. (3) Booster adjuvants as **Keyhole Limpet Hemocyanin (KLH)** which is the key ingredient in the active immunotherapies because it stimulates the immune system against existing disease. (4) Recent advances in dendritic cell cancer vaccination. (5) Cancer-induced immunotolerant pathways such as PD-1/PDL-1 pathway. (6) The role of regulatory T-cells in cancer metastasis.

Dendritic cell (DC) is an antigen presenting cells which play an important role in communication between innate and adaptive immunity [153]. DC can stimulate the two components of adaptive immunity T-cells and B-cells [154]. Improper function of the DC can lead to immune tolerance or autoimmunity [155]. DC is involved in many biological events such as autoimmune diseases, organ transplantation, cancer metastasis, allergic responses and infectious diseases [156]. The DC journey started with its production in bone marrow followed by its settling down in different organs for foreign antigen capturing. Once the foreign antigen is engulfed to DC; it digests it into small peptides and presents them on its surface via major histocompatibility molecules (MHC). Later the DC with the presented antigen will migrate to the nearest lymph node to expose the foreign antigen to T-cell which in turn will adjust the appropriate immune response. The particular T-cell response will depend on the class of presenting molecule on the surface of DC. It is known that the DC expresses both major histocompatibility type I, II (MHC-I & MHC II) [157]. If the antigen is presented by MHC-I, it will attract T-cytotoxic (CD8+), but if the antigen is presented by MHC-II, it will attract T-helper cell (CD4+) [158]. CD8+ T-cell immunity is pathogen-specific, and its responsibility is to encounter the infection and to create memory T-cell which can survive in the absence of foreign antigen to provide sustained protection against recurrent infection [159]. CD4+ T-cell immunity has different pathways depending on its differentiation either into Th1, Th2, Th17, follicular helper T-cell and to T regs [160]. Follicular helper T-cell has the ability to stimulate the proliferation and differentiation of B-cells responsible for antibody production [158]. Treg is responsible for immune suppression or tolerance which is involved in autoimmune disease, organ transplantation, and cancer metastasis. The role of the regulatory T-cells in cancer metastasis was brought to attention since the 1980s. Regulatory T-cells such as CD4+ plays a desired role in inhibiting chronic inflammatory diseases and autoimmune diseases, but regulatory T-cells such as CD25 (+) is involved in undesired cancer metastasis by suppressing the immune system. The administration of anti-CD25 (+) monoclonal antibody decreases the level of regulatory T-cells and the size of the tumor in mice [161]. Recently it was found that immune dysfunction in cancer resulted from neutralization of the killing activity of T-cell in the tumor environment through PD-1/PDL-1 pathway. T-cell expresses PD-1 receptors on its surface which are blocked by PDL-1 ligand overexpressed on transformed cells leading to T-cell inhibition and paralysis. This will protect the cancer cells from the cytotoxic killing activity of T-cell. The discovery of these checkpoints leads to spring out of a new promising class of

anti-cancer drugs targeting PD-1 & PDL-1 which has minimal side effects such as Nivolumab and Atezolizumab [162].

Theranostic polymer nanoparticles—NIR excited upconversion nanoparticles (UCNPs) with dual polymer coating were used to stimulate, mark and track dendritic cells *in vivo*. The UCNPs were synthesized from NaY/GdF₄:Yb:Er (Y:Gd:Yb:Er = 58%:20%:20%:2%). The surface of UCNPs was functionalized with PEG and PEI to form UCNP-PEG-PEI (UPP) dual polymer coated UCNPs. Ovalbumin was used as a model antigen which was loaded onto the polymer surface by electrostatic force. These ovalbumin loaded nanoparticles were successfully loaded into the dendritic cells and induced its maturation associated with potent immune response and increased level of gamma interferon. *In vivo* tracking of UPP antigen-loaded dendritic cells migration to the draining lymph node was carried out by external excitation with 980 nm laser beam. The results showed strong upconversion luminescence (UCL) signals in the nearby lymph node [163].

Theranostic metal nanoparticles—One study was carried out using iron oxide–zinc oxide nanoparticles as antigen delivery agent to dendritic cells. Due to the ability to track iron oxide–zinc oxide nanoparticles *in vitro* and *in vivo* by confocal microscopy and by MRI, respectively. The process of carcinoembryonic antigen loading to dendritic cells was monitored *in vivo* and *in vitro*, and the result showed significant antigen uptake within one hour. An animal study carried on mice bearing tumor showed increased survival rates, suppressed tumor growth, and highly selective T-cell response when compared to control group [164].

Gene delivery

The concept of gene delivery depends on the ability to deliver selective oncogene-blocking agent (DNA or RNA) to transformed cells to downregulate genes responsible for oncogenesis. Delivery of these agents with nanometer scale carrier will increase their potency by several mechanisms such as protection of these agents from enzymatic degradation and delaying of their elimination. Moreover, these agents will be accumulated in the tumor side either by EPR passive targeting or by active targeting thus their genetic translation will be enhanced. The co-delivery of gene therapy and imaging agent has recently become a promising tool to overcome malignancy. The nano-theranostic delivery carrier will be helpful in determining the percent of delivered gene, the efficiency of these knockdown agents, the required concentration for gene silencing and the effectiveness of targeting ligand to direct these agents to only cancerous cells.

Theranostic polymer nanoparticles—Anaplastic thyroid cancer (ATC) is one of the deadly malignancy with a dismal prognosis. ATC is uncommon fastest growing highly aggressive malignancy with a lack of therapeutic response. It has 100% mortality rate with average life expectancy six months. The V-Raf murine sarcoma viral oncogene homolog B (BRAF) is mutated in around 40% of ATC patient, and it is responsible for tumor growth, metastasis, and development of multiple drug resistance. In this study near infrared (NIR) fluorescent polymer is used as a delivering carrier and imaging agent for BRAF- siRNA in ATC orthotropic animal model. The building block polymer was poly [2,6-(4,4-bis-(2-

ethylhexyl)-4H-cyclopenta[2,1-b;3,4-b']dithiophene)-alt-4,7(2,1,3-benzothiadiazole)] (polyPCPDTBT). The result showed 50 nm particle size with extensive tumor homing, delayed renal excretion, efficient gene silencing and tumor restriction [165]. Neuroblastoma is considered the second leading solid tumor in children with poor prognosis and negligible recovery percent. Here is a targeted polymer nanotheranostic carrier developed to target neuroblastoma. This nanosystem is composed poly (D,L-lactide-*co*-glycolide) (PLG) polymer carrier, rabies virus glycoprotein (RVG) as a targeting ligand to neuroblastoma, fluorescein isothiocyanate (FITC) as a fluorescent imaging agent and a mixture of gene therapy composed of (siMyc, siBcl-2, and siVEGF) as tumor suppressor therapy. The result concluded that this formulation is selectively target neuroblastoma both *in vivo* and *in vitro*. The animal study showed enhancement in formulation tracking, tumor follows up and a promising suppression of tumor proliferation [166].

Theranostic metal nanoparticles—One study was carried out to deliver PD-L1 knocking down siRNA and imaging agent to gastric cancer. PD-L1 is responsible for the failure of cancer immune therapy and development of immune tolerance via interacting with PD-1 in T-cells. PD-L1 knocking down siRNA was delivered to cancer cells through folate decorated nanoparticle as folate is overexpressed in some cancer subtypes. The nanoparticle composed of Folic acid (FA)/Disulfide (SS)/Polyethyleneglycol (PEG)/Polyethyleneimine (PEI)/Superparamagnetic iron oxide Fe₃O₄ nanoparticles (SPIONs). The siRNA was loaded to FA-PEG-SS-PEI-SPIONs to form polyplex with 120 nm diameter. The folate-targeted nanoparticles showed high cellular uptake and increased transfection potency in folate receptor overexpressing gastric cancer cell line (SGC-7901) when compared to non-targeted nanoparticles. MRI carried on the cellular level proved the ability to use this polyplex as a nanoprobe for cancer diagnosis. It was concluded that this nanoplatform is able to down-regulate PD-L1 in both gene and protein level [167]. Another study aimed to down-regulate survivin gene in hepatocellular carcinoma (HCC) to enhance cellular apoptosis. The nanoparticle design was constructed by using amylose as fundamental nano-carrier coated with superparamagnetic iron oxide and decorated with folate targeting molecule to HCC cells. The result showed that these nanoparticles could selectively deliver siRNA with effective down-regulation of survivin gene in HCC cells which hold a great promise for the development of theranostic gene carrier [168]. A new approach to combine both photothermal therapy, gene therapy and tumor imaging agent was studied by manufacturing of gold nanostar (AU NS) stabilized by a certain dendrimer. This vehicle was used as VEGF-siRNA cargo to a cancerous cell. The result showed that the siRNA was effectively delivered to tumor cells and when combined with near infra-red laser beam the viability was around 20.2% which was better than the result obtained from individual gene or photothermal therapy [169]. All the theranostic NPs that have been extensively illustrated in the previous sections are summarized in Table 2.

Toxicity and limitations associated with theranostic nanoparticles

The primary aim of delivering drugs within NPs carrier is to reduce the associated systemic toxicity. Recently the application of nanotechnology has been grown on in all medical and scientific levels; so extensive studies and vigorous research are required to address their

therapeutic safety margin and their toxicity. Many studies have been established to investigate their immunotoxicity and genotoxicity in addition to the impact of their application on the cell viability, cell membrane vitality, and inflammatory response. Detecting the toxicity associated with NPs is challenging due to lack of the proper detecting methods, so it is an urgent need to develop accurate, valid techniques to predict their future side effects, especially by animal models. FDA has paid considerable attention to set strict regulations for using NPs based on their therapeutic outcomes versus their cumulative toxicity [172].

Theranostic polymer nanoparticles

More often, because the majority of the polymers used as vehicles are biodegradable, they are degraded on the release of the drug payload, thus, affording degradation products that are not toxic to the body. In general, polymer NPs seem to have no warning signs, no adverse immune side effect. One of the FDA approved polymer NPs which is considered safe right now is the poly-(D,L-lactide-co-glycolide) (PLGA) because it hydrolyzes to lactic acid and glycolic acid which are deemed to be natural biological metabolite [173]. On the other hand coating of PLGA NPs with charged stabilizers have shown unexpected dose-dependent cellular cytotoxicity to THP-1 macrophages, increasing the apprehension towards using stabilizer [174]. Another polymer named polybutylcyanoacrylate nanoparticles (PBCA NPs) labeled with rhodamine and injected in rats were deemed safe and non-toxic even at high doses [175]. Even it is a customary practice to coat the surface of NPs with polyethylene glycol (PEG) to increase the circulation time of the NPs *in vivo*, increase the NPs stability and mask the biomolecules from trapping by RES [176] and even there are a lot of PEGylated pharmaceutical drugs have been FDA approved, a great attention is directed to their recent limitations. It is reported that PEG is non-degradable and immunogenic. Many studies reported the presence of anti-PEG antibodies in animal models and patients treated with various PEGylated agents [177]. It is also important to notice that the non-human therapeutic peptides and proteins are immunogenic *per se* when administrated in human. In one study rabbits were immunized with PEGylated ovalbumin and PEG alone. The results showed a high immunogenic reaction to PEGylated ovalbumin while no immunogenic reaction to PEG alone [178]. Sever systemic toxicity associated with high level of IgE was reported in patient received PEGylated corticoid [179]. Also, it is noticed that the percent of anti-PEG antibodies especially IgG and IgM isotypes is increasing in the serum of healthy blood donors due to the growing exposure of the general population to PEG in pharmaceutical products in recent years [180]. The coexistence of these anti-PEG antibodies adversely affects the therapeutic efficacy of many PEGylated drugs and increases their clearance such as PEG-asparaginase, the drug for acute lymphoblastic leukemia [180]. Rigorous investigations are going on to replace the PEG with other non-immunogenic degradable stabilizers such as naturally degradable polysaccharides or synthetic degradable polymers such as zwitterions. Zwitterions are neutral polyelectrolytes which have been developed recently as a promising alternative class to prevent protein adsorption on the surface of NPs. Three types of zwitterions are under investigation, namely, carboxybetaine, phosphocholine, and sulfobetaine. Many studies have been carried out to compare between the well-established PEG coating and the new emerging zwitterions alternative from many aspects such as affinity, stability, mechanism of action and immunogenicity. One of those

studies was carried on magnetic iron oxide NPs. The study compares between the zwitterionic dopamine sulfonate (ZDS) coated MNPs, and PEG-like 2-[2-(2-methoxyethoxy)ethoxy]-acetic acid (MEEA) coated MNP. The result showed the ZDS coated NPs were stable, non-aggregable when compared to MEEA coated NPs [181]. Also, it was reported that the zwitterions are better than PEG in therapeutic coating because they do not generate polymer specific antibodies [182].

Theranostic metal nanoparticles

Despite the diagnostic advantages of metal nanoparticles over polymer, there are several reports published about the cytotoxicity of the former *in vitro* and *in vivo*. Iron oxide nanoparticles tend to accumulate in the liver. However, this has served to its advantage in a way that they can be excellent candidates for imaging in diseased liver tissue. Though iron oxide and gold nanoparticles have made their way through approval to the market, there is still skepticism regarding their widespread use in clinics. An *in vitro* study in murine macrophage cells was carried about the safety of superparamagnetic iron oxide nanoparticles (SPIONs) at high concentrations, concluding that it is imperative to use SPIONs at low levels to avoid cell death associated with induction of oxidative stress [183]. *In vitro*, bare SPIONs are often more cytotoxic than SPIONs coated with dextran, citrate, etc. Several studies have also reported the mitochondrial damage due to the generation of ROS, lipid peroxidation and inflammatory response by coated SPIONs [184]. The *in vivo* toxicities of SPIONs are generally very mild and occur only for short duration like diarrhea, nausea, though the toxicities at high doses that include DNA damage and possible initiation of carcinogenesis cannot be neglected [185]. Another toxicological study proved improvement in therapeutic safety margin of the polymer encapsulated DOX-Ps 80-SPIONs when compared to free DOX confirmed by hematoxylin and eosin stain (H&E) pathological screening of cardiac muscle as it is known that cardiac toxicity is the most common adverse effect of DOX. The reticuloendothelial contributing tissues including hepatic, spleen, pulmonary and renal sections were also screened because it is known that they are the most common sites for nanoparticles trapping as illustrated in Fig. 9. Non-detectable cardiac toxicity with minor changes in the RES for the encapsulated DOX when compared with severe cardiac toxicity and significant changes of RES for free DOX when given to glioma-bearing rats in equivalent doses. Then it is predicted that polymer coating reduces the toxicity of DOX and SPIONs [117]. Interestingly, there has been evidence of size-dependent toxicities of metal nanoparticles. It has been shown that 1.5 nm gold nanoparticles are more toxic than those at 15 nm. Moreover, while neutral gold nanoparticles are reportedly 'nontoxic,' cationic gold nanoparticles are deemed to be toxic. Some others have reported the severity of oxidative damage because of gold nanoparticles despite their popularity concerning market dominance [186]. Also, it was reported that there are time and dose-dependent genotoxicity associated with zinc oxide nanoparticles with a concomitant increase in tyrosine phosphorylation level [187]. Manganese oxide is not out of criticism as it was reported that the inhalation of its nanoparticles in rats was associated with acute toxicity characterized by respiratory apnea and neurological manifestation [188]. Despite the reports surrounding cellular damage and apoptosis because of metal nanoparticles, their participation in the theranostic domain is highly acclaimed and dominated over other classes of theranostics (Table 3).

Illustrative patents on polymer and metal theranostic nanoparticles

Many publications are demonstrating the novelty of theranostic polymer and metal NPs over the past few decades. Each of them unraveling a multitude of possibilities in improving the existing ones. We have presented, in this review, a brief section on the aspect of commercialization of theranostics since this will ultimately dictate the feasibility of clinical translation of the developed product. Thus, here are some of the recorded patents of polymer and metal theranostic NPs which could be synthesized either separately or combined.

A wide variety of theranostic NPs employ biocompatible polymers as the drug carrier and either a metal or fluorescent dye as the diagnostic moiety. Metal theranostic NPs have also been patented under a wide domain, thanks to the larger variety of metals that have a documented safe and effective diagnostic potential. In the patent US8236284 B1,⁵ polymer and metal bases were merged in one formulation. The formulation was composed of superparamagnetic iron oxide core and a polyacrylic acid polymer shell. The polymer shell has an outer hydrophilic side suitable for ligand conjugation and inner hydrophobic side ideal for lipophilic fluorescent dye and drug encapsulation [196]. In parallel, patent US20130323165 A1 gives a detailed description about enclosing of paramagnetic, radiolabeled, fluorophores, and/or emission tomographic agents into a single biologically compatible carrier and the feasibility to use the entire formulation as a multi-functional theranostic platform [197]. In the patent US20170014531 A1, a smart stimuli-responsive polymeric system was registered. The system was composed of a fluorescent imaging agent and a therapeutic agent attached to the polymer based on their solubility. The strength of the generated fluorescence signal is dependent on the intensity of a catalyst stimulus which is over-expressed in the diseased tissue [198]. The patent US20140037542 A1 talks about encapsulating quaterrylene dye in a dendrimer shell to be used as a theranostic delivery boat. The surface can be functionalized with a target ligand for cancer delivery purpose. It can be used for delivering a therapeutic agent or imaging agent or both of them. Also, it can be used for real-time monitoring of disease elimination [199]. In the patent US20130039858 A1, metal oxide NPs were used with a fluorescent dye which can bind to the former either covalently or ionically. Surface functionalization enhances the theranostic application of these NPs *in vivo* or *in vitro*. The utility of combining thermal therapy with these NPs was also recorded [200]. Patent US9248441 B2 talks about the ability of polymer nano-capsules to enclose theranostic metal. The imaging metal could be gold, silver, palladium or platinum [201]. Patent US20160303257 A1 discusses the application of enzyme-responsive theranostic NPs. It focuses on the ability of MMP-14 enzyme which is overexpressed in the tumor microenvironment to degrade the theranostic carrier and release iron oxide contrasting agent [202]. Patent EP 1651957 discusses the preparation of NPs with a magnetic and fluorescent core and phosphor fluoride shell to be applied as markers in biological assays [203]. Patent EP2277548 B1 invests in a similar logic, describing NPs with a magnetic core with specific ligands immobilized onto their surfaces [204].

The number of patents around theranostic nanoparticles not only convinces us of its evolving market potential but also reaffirms our belief into investing scientific expertise for

⁵<https://patents.google.com/patent/US8236284B1/en?q=US8236284+B1>.

developing advanced modular platforms that can serve both therapy and diagnosis together. So far, we have briefed only a minuscule number of patents in the theranostic domain that are representative of the major design of theranostics. Nevertheless, there always remains a lot more to be read for an interested reader.

Demonstrative clinical trials on polymer and metal theranostic nanoparticles

Polymer nanoparticles

ThermoDox is a heat-responsive liposome which has completed phase III clinical trials (). It was started in May 2008 and completed in August 2016 under the title “Phase 3 Study of ThermoDox With Radiofrequency Ablation (RFA) in Treatment of Hepatocellular Carcinoma (HCC)”. It is an interventional-type clinical trial with 701 participants. Patients were split into two groups; the control group received 5% dextrose solution as a single intravenous infusion lasted for 30 min and the treated group received ThermoDox 50 mg/m² as a single intravenous infusion lasted for 30 min. The RFA started 15 min after starting the infusion and completed within 3 h after starting the infusion. The length of exposure to RFA depends on the tumor size. CT imaging was used to assess the effectiveness of the RFA therapy. TARDOX is a completed phase I clinical trials (). It was started in July 2014 and completed in April 2017 under the title “Targeted Chemotherapy Using Focused Ultrasound for Liver Tumours (TARDOX).” It is an interventional-type clinical trial with 10 participants. The study aims to investigate the feasibility of using focused ultrasound (FUS) to enhance the release of doxorubicin from lyso-thermosensitive liposomal (LTSL) into liver cancer. The patients received treatment for one day and were followed up for 30 days. The therapeutic effect on the tumor was monitored within 60 days of intervention by MRI, CT, and FDG PET-CT scan. The results were successful, promising and potentiate the large-scale clinical translation. One of liposome-based DC vaccine in phase I clinical trials is DepoVaxTM (DPX-0907). It consists of liposomal carrier for both TAAs (Human leukocyte antigen (HLA)-A2) and adjuvant. This aqueous liposomal formulation was adjusted to 120 nm by an extruder, lyophilized, stored at 4 °C and re-suspended with Montanide ISA51 VG just before injection. It was found that this type of vaccination when tested on advanced cases of breast, ovarian and prostate cancer showed efficient trapping of DCs to the site of injection, the antigen was uptaken and presented by antigen presenting cells, production of peptide-specific T-cells, significant immune response after single injection, generation of memory T-cell with high safety margin owing to using tumor-specific antigen, producible, stable and storable [205]. The aim of the aforementioned three studies was treatment, but as it is discussed through the manuscript, the liposome NPs is convenient for theranostic application too.

Metal nanoparticles

An active phase I clinical trial () that started in November 2015 and estimated to be completed in November 2019 under the title “Theranostics of Radiolabeled Somatostatin Antagonists 68Ga-DOTA-JR11 and 177Lu-DOTA-JR11 in Patients with Neuroendocrine Tumors”, is an interventional-type clinical trial with an actual enrolment of 20 patients.

Radiolabeled somatostatin antagonists were used in the study as the imaging and therapeutic tool for metastatic neuroendocrine tumors. In this trial, a small protein called DOTA-JR11 was used as a targeting ligand to bind to overexpressed somatostatin receptors on the neuroendocrine tumor cells. Radioactive substances ^{68}Ga and ^{177}Lu were attached to DOTA-JR11 for diagnosis and therapy respectively. ^{68}Ga -DOTA-JR11 with PET/CT light up in tumor tissue helping the doctors to find out the tumor. Then patients received ^{177}Lu -DOTA-JR11, upon reaching the tumor side the ^{177}Lu radioactive substance will kill the cancerous cell by the aid of radiation. The aforementioned intervention was to be delivered in 2 cycles, approximately 3 months apart. Another phase II active clinical trial () under the title “Theranostics: ^{68}Ga DOTATOC and ^{90}Y DOTATOC (PRRT)” is an interventional-type clinical trial with 25 participating patients. The study started in May 2015 and expected to be completed in October 2020 aims to diagnose and treat the somatostatin-expressing tumors such as a neuroendocrine tumor, medulloblastoma, meningioma, and neuroblastoma. ^{68}Ga -DOTATOC PET/CT is used to detect cancer and measure the degree of responsiveness to ^{90}Y -DOTATOC therapy. The treatment arm comprises of a radiopharmaceutical, ^{90}Y -DOTA-tyr3-Octreotide that is combined with a renal protectant, Aminosyn II which limits the dose of the radiopharmaceutical in the kidney. The intervention was to be administered in 3 intravenous doses with 6 weeks apart.

Conclusion

Theranostic nanoparticle field has witnessed growing progress in disease management. Since the last decade, various kinds of polymer and metal theranostic nanoparticles have been utilized for simultaneous cancer imaging and therapy with promising preclinical outcomes. Despite the significant advances in theranostic NPs field such as active targeting to the tumor site, development of stimuli-responsive nanoparticles, the feasibility of therapeutic combination, the possibility of applying controlled-release approach and improving the therapeutic outcomes by photothermal therapy or magnetic field, many difficulties still limit its clinical success. An interdisciplinary approach is required to overcome these limitations and to enhance their personalized medicine application. Many parameters need to be optimized before large-scale clinical translation such as drug encapsulation, ligand conjugation efficiency, safety and carrier biodegradability. Also, high reproducibility with uncostly materials is an essential issue for clinical application. In this review, several types of polymer and metal nanoparticles employed for the theranostic approach in cancer management have been discussed with insightful pointing to their limitations and future applications. Also, the impact of the tumor microenvironment on the biodistribution of nanoparticles has been addressed. Moreover, this review discusses many available promising alternatives to overcome some of the faced limitations such as using affibody to improve targeting efficiency, application of zwitterionic agents to overcome polymer immunogenicity and active targeting of the NPs used for neurological disorders with transferrin or lactoferrin to overcome blood–brain barrier.

Acknowledgments

GN would like to thank the Culture Affairs and Mission Sector, Ministry of Higher Education, Government of Egypt for the Ph.D. scholarship in Iyer lab, Wayne State University. The authors wish to acknowledge Mr. Rami Alzharni, Mr. Hashem Obaid Alsaab, and Katyayani Tatiparti for their technical support and valuable suggestions.

AKI would like to acknowledge NCI/NIH (R21CA179652), Wayne State University Start-up and American Cancer Society (ACS-IRG#449355) for funding support.

Appendix A.: List of abbreviation

Abbreviation	Clarification
A-549	Lung cancer
Ag NC	Silver nanocluster
AFP	α -fetoprotein
AIDS-KS	AIDS-related Kaposi sarcoma
5-ALA	5-aminolevulinic acid
AO	Acridine orange
ATC	Anaplastic thyroid cancer
AU NS	Gold nanostar
Bcl-2	Antiapoptotic B cell lymphoma-2
bFGF	Basic fibroblast growth factor
BRAF	It is a human gene code for B-Raf protein. The gene is also known V-Raf murine sarcoma viral oncogene homolog B.
BxPC-3	Pancreatic cancer cells
C6 glioma	Glioma cell line
CAC	Critical aggregation concentration
Caco-2	Colorectal adenocarcinoma cell line
CAFs	Cancer-associated fibroblasts
CDF	3,4-difluorobenzylidene-curcumin
CdSe	Cadmium selenide
CdTe	Cadmium telluride
CF488	Green fluorescent dye
CLSM	Confocal laser scanning microscope
CNS	Central nervous system
CT	Computed tomography
⁶⁴ Cu	Copper-64 radioisotopes
DDS	Drug delivery system
DiR	1,1'-Diocadecyl-3,3,3',3'-tetramethylindotricarbocyanine Iodide
DLS	Dynamic light scattering
DNA	Deoxyribonucleic acid
DOX	Doxorubicin
DPPC	1,2-dipalmitoyl-sn-glycero-3-phosphocholine
DSPC	1,2-distearoylglycero-3-phosphocholine
DSPE-mPEG-2000	1,2-distearoyl-sn-glycero-3-phosphoethanolamine-N-[methoxy(polyethylene glycol)-2000]
DU145	Androgen insensitive prostate cancer cell line
Dunning AT1	Prostate tumor cells
EB	Ethidium bromide
EG	Poly (ethylene glycol)-b-Poly (glutamic acid)
EGFR	Epidermal growth factor receptor

Abbreviation	Clarification
EMC	Extracellular matrix component
EPR	Enhanced permeability and retention
Er	Erbium
FA	Folic Acid
FACS	Fluorescence-activated cell sorting
FDA	Food and drug administration
FITC	Fluorescein isothiocyanate
5-FU	Fluorouracil
Ga 68	Gallium-68
GAGs	Glycosaminoglycans
GEG	Poly (ethylene glycol)-b-poly (glutamic acid)-b-poly (ethylene glycol)
Gd	Gadolinium
Gd-DTPA	Gadolinium diethylenetriamine pentacetic acid
GdF ₄	Gadolinium fluoride
GRE	Glucocorticoid responsive element
GRP78	Glucose-regulated protein of 78 kDa
GSH	Glutathione
HA	Hyaluronic acid
HAMA	Human anti-mouse antibody
HCC	Hepatocellular carcinoma
H&E	Hematoxylin and eosin stain
HeLa	Human cervical carcinoma
HER2	Human epidermal growth factor Receptor 2
HIFU	High-intensity focused ultrasound
HOOC-PEG3.4k-PCL15k	α -carboxyl poly(ethylene glycol)-poly (ϵ -caprolactone)
HPMA	<i>N</i> -(2-hydroxypropyl)methacrylamide
HU	Hounsfield unit
ICG	Indocyanine green
IDLPL	¹¹¹ In-DTPA-labeled pegylated liposomes
IFP	Interstitial fluid pressure
IgG	Immunoglobulin G
IGROV-1	Ovarian cancer cells
InAs	Indium arsenide
InP	Indium phosphide
IONPs	Magnetic iron oxide nanoparticles
LSPR	Localized surface plasmon resonance
¹⁷⁷ Lu	Lutetium-177
MCF 7	Breast cancer cell line
MDR	Multidrug resistance
MEEA	2-[2-(2-methoxyethoxy)ethoxy]-acetic acid
MMP	Matrix metalloproteinase
MNPs	Magnetic nanoparticle

Abbreviation	Clarification
Mn ²⁺	Manganese ion
MPEG3k-PCL15k	Methoxy poly(ethylene glycol)-poly (ϵ -caprolactone)
MRI	Magnetic resonance imaging
^{99m} Tc	Technetium-99m: it is an isotope of technetium
MTX	Methotrexate
Myc	Regulator gene that codes for a transcription factor
NCPs	Nanoscale coordination polymer
NCT	Neutron capture therapy
NIR	Near-infrared dye
NIS	Sodium iodide symporter gene
NP	Nanoparticles
OVCAR3	Ovarian carcinoma cells
PAMAM	Poly (amidoamine)
PBCA NPs	Polybutylcyanoacrylate Nanoparticles
PC-3	Androgen insensitive prostate cancer cell line
PDA	Polydopamine
PDAC	Pancreatic ductal adenocarcinoma
PDGF	Platelet-derived growth factor
PD-L1	Programmed death-ligand 1
SPD-1	Programmed death-1
PDT	Photodynamic therapy
PEI	Polyethyleneimine
PEG	Polyethylene glycol
PET	Positron emission tomography
PLA-PEG	Poly(lactic acid)-co-Poly(ethylene glycol)
PLGA	Poly-(D,L-lactide-co-glycolide)
PLG	Poly (D,L-lactide-co-glycolide)
PolyPCPDTBT	Poly[2,6-(4,4-bis-(2-ethylhexyl)-4H-cyclopenta [2,1-b;3,4-b']dithiophene)-alt-4,7(2,1,3-benzothiadiazole)]
Ps 80	Polysorbate 80
QD	Quantum dots
RES	Reticuloendothelial system
RF	Radiofrequency
RNA	Ribonucleic acid
RbCur	Boron-curcumin complex
ROS	Reactive oxygen species
RVG	Rabies virus glycoprotein
SC	Stratum corneum
SCC	Human squamous cell carcinoma
SDF-1	Stroma-derived factor
SGC-7901	Gastric cancer cell line
SKOV3	Ovarian carcinoma cells

Abbreviation	Clarification
SPECT	Single-photon emission computed tomography
SPIONs	Superparamagnetic iron oxide nanoparticles
SRB	Sulforhodamine B protein-dye
SS	Disulfide bond
T2/T1	Relaxation time
TDD	Transdermal drug delivery
TEM	Transmission electron microscopy
Tet	Tetrandrine
TGF- β	Transforming growth factor beta
THP-1	Human monocytic cell line
TME	Tumor microenvironment
TPP	Triphenylphosphonium cation
TRC105	Carotuximab
TSL	Temperature-sensitive liposome
U-87	Brain cancer
UCL	Upconversion luminescence
UCNPs	Upconversion nanoparticles
uPA	Urokinase plasminogen activator
uPAR	Urokinase plasminogen activator receptor
VEGF	Vascular endothelial growth factor
Y	Yttrium
Yb	Ytterbium
ZDS	Zwitterionic dopamine sulfonate

Biographies

Ms. Ghazal Nabil is an assistant lecturer in Pharmacology Department, Faculty of Veterinary Medicine, Cairo University. She got her Bachelor's degree in 2010 and Master degree in Pharmacology in 2013 from the faculty of Veterinary Medicine, Cairo University, Egypt. Currently, she is a Ph.D. student co-mentored by Dr. El Banna at Cairo University, Egypt and Dr. Iyer lab at Wayne State University, Detroit, Michigan, USA. She joined Wayne State University as a part of her joint mission entitled "the application of the nanomedicine in the field of oncology" which is fully funded by the Egyptian government.



Ms. Ketki Bhise is currently a PhD student in Dr. Iyer lab at Wayne State University, Detroit, Michigan, USA. She has completed her Master's degree in Pharmaceutical Sciences and Technology from Institute of Chemical Technology (ICT), Mumbai, India in the year 2016. Her Master's thesis was on the Quality by Design based approach in development and

evaluation of nanostructured lipid carriers for the co-delivery of two potent anticancer agents derived from natural sources. Her Bachelor's degree in Biotechnology Engineering was from Savitribai Phule Pune University, Pune, India, wherein she had worked on the extraction, quantification and purification of Safranal obtained from different plant sources.



Dr. Samaresh Sau is a senior research scientist in the Department of Pharmaceutical Science in Wayne State University, USA. He received his PhD from CSIR-Indian Institute of Chemical Technology, India and then pursued his first postdoctoral training at Purdue University, USA. His research is focused on developing clinically translatable nanoparticle, small molecule drug delivery system and immune therapy for cancer. He has more than 30 international publications, 2 U.S pending patents, and 2 federal and private grants.



Mohamed Atef Ahmed Shehata He is one of the greatest pharmacological scientists in Egypt. He is a professor in the Pharmacology Department, Faculty of Veterinary Medicine, Cairo University and he is one of the founders of the pharmacology department. He was a Vice Dean for higher education in the Faculty of Veterinary Medicine, Cairo University. His research areas of interests are to evaluate the pharmacological activities of medicinal plants, monitor the pharmacokinetics of chemotherapeutic agents such as the antibiotics and anthelmintics in a various animal model, and check the impact of many compounds in the male and female fertility. He has at least 150 published papers in prestigious journals. He supervised more than 80 master and Ph.D. students all over Egypt and Middle Eastern countries. Dr. Atef was awarded Country Honoring Award, University Award of Excellence and many other reputable awards all over the country. He attended more than 70 conferences. He is currently a reviewer for many journals in the field of pharmacology. Also, He has been invited as a speaker at many international conferences.



Dr. Hossny El Banna is a professor and head of the Pharmacology Department, Faculty of Veterinary Medicine, Cairo University since 2000. He was a Vice Dean for Education, and Student Affairs for the Faculty of Veterinary Medicine, Cairo University. His research interests are to evaluate the pharmacological activities of medicinal plants and

pharmacokinetics of chemotherapeutic agents. He has published more than 60 peer-reviewed journals and 50 conference papers. Dr. El Banna has been invited as a speaker at many international conferences and he has supervised more than 25 Master's and Ph.D. students from different nations.



Dr. Iyer is the Director of U-BiND Systems Laboratory and Assistant Professor of Pharmaceutical Sciences at Wayne State University, Detroit, Michigan, USA. Dr. Iyer received his PhD at Sojo University, Japan, under Professor Hiroshi Maeda (2016 Nobel Prize in Chemistry Nominee). Dr. Iyer is a US DoD Early Career Investigator and recipient of the prestigious CRS T. Nagai Research Achievement Award. Dr. Iyer has authored >100 publications in peer reviewed International Journals and books and has wide expertise in biomaterials and nanomedicine for treating diseases such as infection, inflammation and cancer. His laboratory is funded by agencies such as NIH, DoD, American Cancer Society and private foundations.



References

1. Ventola CL et al. (2010) The nanomedicine revolution: part 1: emerging concepts. *Pharmacy and therapeutics*. *Pharmacol. Ther* 128, 512–525. 10.1016/j.pharmthera.2010.07.007
2. Bhise K et al. (2017) Nanomedicine for cancer diagnosis and therapy: advancement, success and structure–activity relationship. *Ther. Deliv* 8, 1003–1018. 10.4155/tde-2017-0062 [PubMed: 29061101]
3. Luong D et al. (2017) Polyvalent folate-dendrimer-coated iron oxide theranostic nanoparticles for simultaneous magnetic resonance imaging and precise cancer cell targeting. *Biomacromolecules* 18 (4), 1197–1209. 10.1021/acs.biomac.6b01885 acs.biomac.6b01885 [PubMed: 28245646]
4. Lu Z (2014) *Theranostics Fusion of Therapeutics and Diagnostics*. 2014
5. Peng H et al. (2015) Polymeric multifunctional nanomaterials for theranostics. *J. Mater. Chem. B* 3, 6856–6870. 10.1039/C5TB00617A
6. Xie J et al. (2010) Nanoparticle-based theranostic agents. *Adv. Drug Deliv. Rev* 62, 1064–1079. 10.1016/j.addr.2010.07.009 [PubMed: 20691229]
7. Janib SM et al. (2010) Imaging and drug delivery using theranostic nanoparticles. *Adv. Drug Deliv. Rev* 62, 1052–1063. 10.1016/j.addr.2010.08.004 [PubMed: 20709124]
8. Shah L et al. (2015) *Targeted Drug Delivery: Concepts and Design*. 2015. 10.1007/978-3-319-11355-5
9. Iyer AK et al. (2012) Image-guided nanosystems for targeted delivery in cancer therapy. *Curr. Med. Chem* 19, 3230–3240. 10.2174/092986712800784685 [PubMed: 22612697]
10. Fang J et al. (2007) Tumor-targeted induction of oxystress for cancer therapy. *J. Drug Target*. 15, 475–486. 10.1080/10611860701498286 [PubMed: 17671894]

11. Abeylath SC et al. (2011) Combinatorial-designed multifunctional polymeric nanosystems for tumor-targeted therapeutic delivery. *Acc Chem. Res* 44, 1009–1017. 10.1021/ar2000106 [PubMed: 21761902]
12. Iyer AK and Ave M (2016) Rational Design of Multifunctional Nanoparticles for Targeted Cancer Imaging and Therapy. 2016609–656
13. Mukherjee S et al. (2016) Green synthesis and characterization of monodispersed gold nanoparticles: toxicity study, delivery of doxorubicin and its bio-distribution in mouse model. *J. Biomed. Nanotechnol* 12, 165–181. 10.1166/jbn.2016.2141 [PubMed: 27301182]
14. Sau S et al. (2014) Cancer cell-selective promoter recognition accompanies antitumor effect by glucocorticoid receptor-targeted gold nanoparticle. *Nanoscale* 6, 6745–6754. 10.1039/c4nr00974f [PubMed: 24824564]
15. Sahu P et al. (2017) Assessment of penetration potential of pH responsive double walled biodegradable nanogels coated with eucalyptus oil for the controlled delivery of 5-fluorouracil: in vitro and ex vivo studies. *J. Control. Release* 253, 122–136. 10.1016/j.jconrel.2017.03.023 [PubMed: 28322977]
16. Haley B and Frenkel E (2008) Nanoparticles for drug delivery in cancer treatment. *Urol. Oncol. Semin. Orig. Investig* 26, 57–64. 10.1016/j.urolonc.2007.03.015
17. Sahu P et al. (2017) pH Responsive biodegradable nanogels for sustained release of bleomycin. *Bioorg. Med. Chem* 25 (17), 4595–4613. 10.1016/j.bmc.2017.06.038 [PubMed: 28734664]
18. Anjibabu R et al. (2013) Heteropoly acid catalyzed synthesis of 8-methyl-2-aryl/alkyl-3-oxabicyclo[3.3.1]non-7-ene derivatives through (3,5)-oxonium-ene reaction. *Tetrahedron Lett.* 54, 7160–7163. 10.1016/j.tetlet.2013.10.103
19. Ganapathy V et al. (2015) Targeting tumor metastases: drug delivery mechanisms and technologies. *J. Control. Release* 219, 215–223. 10.1016/j.jconrel.2015.09.042 [PubMed: 26409123]
20. Alsaab H et al. (2017) Folate decorated nanomicelles loaded with a potent curcumin analogue for targeting retinoblastoma. *Pharmaceutics* 9, 15 10.3390/pharmaceutics9020015
21. Jo SD et al. (2016) Targeted nanotheranostics for future personalized medicine: recent progress in cancer therapy. *Theranostics* 6, 1362–1377. 10.7150/thno.15335 [PubMed: 27375785]
22. Lucas S et al. (2017) Pharmacological inhibitors of NAD biosynthesis as potential anticancer agents. *Recent Pat. Anticancer Drug Discov.* 12 (3), 190–207. 10.2174/1574892812666170619125503 [PubMed: 28637419]
23. Sharma B and Kanwar SS (2017) Phosphatidylserine A cancer cell targeting biomarker. *Semin. Cancer Biol.* 52 (Pt. 1), 17–25. 10.1016/j.semcancer.2017.08.012 [PubMed: 28870843]
24. Schwartz JA et al. (2009) Feasibility study of particle-assisted laser ablation of brain tumors in orthotopic canine model. *Cancer Res.* 69, 1659–1667. 10.1158/0008-5472.CAN-08-2535 [PubMed: 19208847]
25. mejkalová D et al. (2014) Selective in vitro anticancer effect of superparamagnetic iron oxide nanoparticles loaded in hyaluronan polymeric micelles. *Biomacromolecules* 15, 4012–4020. 10.1021/bm501065q [PubMed: 25268047]
26. Gao N et al. (2017) Tumor penetrating theranostic nanoparticles for enhancement of targeted and image-guided drug delivery into peritoneal tumors following intraperitoneal delivery. *Theranostics* 7, 1689–1704. 10.7150/thno.18125 [PubMed: 28529645]
27. Chen Y et al. (2012) Preparation of curcumin-loaded liposomes and evaluation of their skin permeation and pharmacodynamics. *Molecules* 17, 5972–5987. 10.3390/molecules17055972 [PubMed: 22609787]
28. Shi H et al. (2015) A smart all-in-one theranostic platform for CT imaging guided tumor microwave thermotherapy based on IL@ZrO₂ nanoparticles. *Chem. Sci* 6, 5016–5026. 10.1039/C5SC00781J [PubMed: 30155006]
29. Truzzi E et al. (2017) Self-assembled lipid nanoparticles for oral delivery of heparin-coated iron oxide nanoparticles for theranostic purposes. *Molecules* 22, 963 10.3390/molecules22060963
30. Kuzmov A and Minko T (2015) Nanotechnology approaches for inhalation treatment of lung diseases. *J. Control. Release* 219, 500–518. 10.1016/J.JCONREL.2015.07.024 [PubMed: 26297206]

31. Iyer AK et al. (2006) Exploiting the enhanced permeability and retention effect for tumor targeting. *Drug Discov. Today* 11, 812–818. 10.1016/j.drudis.2006.07.005 [PubMed: 16935749]
32. Drugs A (2006) *Delivery of Protein and Peptide Drugs in Cancer*. pp. 1–392, Imp Coll Press
33. Greish K (2007) Enhanced permeability and retention of macromolecular drugs in solid tumors: a royal gate for targeted anticancer nanomedicines. *J. Drug Target.* 15, 457–464 [PubMed: 17671892]
34. Akhtari J et al. (2016) Targeting, bio distributive and tumor growth inhibiting characterization of anti-HER2 affibody coupling to liposomal doxorubicin using BALB/c mice bearing TUBO tumors. *Int. J. Pharm* 505, 89–95. 10.1016/j.ijpharm.2016.03.060 [PubMed: 27039149]
35. Lammers T et al. (2011) Theranostic nanomedicine. *Acc. Chem. Res* 44, 1029–1038. 10.1021/ar200019c [PubMed: 21545096]
36. Matsumura Y and Maeda H (1986) A new concept for macromolecular therapeutics in cancer chemotherapy: mechanism of tumorotropic accumulation of proteins and the antitumor agents smancs. *Cancer Res.* 46, 6387–6392. 10.1021/bc100070g [PubMed: 2946403]
37. Nakamura Y et al. (2016) Nanodrug delivery is the enhanced permeability and retention effect sufficient for curing cancer? *Bioconj. Chem* 27, 2225–2238. 10.1021/acs.bioconjchem.6b00437 [PubMed: 27547843]
38. McDonald DM et al. (1999) Endothelial gaps as sites for plasma leakage in inflammation. *Microcirculation* 6, 7–22. 10.1111/j.1549-8719.1999.tb00084.x [PubMed: 10100186]
39. Yurchenco PD and Ruben GC (1987) Basement-membrane structure in situ — evidence for lateral associations in the type-IV collagen network. *J. Cell Biol.* 105, 2559–2568. 10.1083/jcb.105.6.2559 [PubMed: 3693393]
40. Kanapathipillai M et al. (2014) Nanoparticle targeting of anti-cancer drugs that alter intracellular signaling or influence the tumor microenvironment. *Adv. Drug Deliv. Rev* 79, 107–118. 10.1016/j.addr.2014.05.005 [PubMed: 24819216]
41. Baluk P et al. (2003) Abnormalities of basement membrane on blood vessels and endothelial sprouts in tumors. *Am. J. Pathol* 163, 1801–1815. 10.1016/S0002-9440(10)63540-7 [PubMed: 14578181]
42. O'Brien MER et al. (2004) Reduced cardiotoxicity and comparable efficacy in a phase III trial of pegylated liposomal doxorubicin HCl (CAELYX/Doxil) versus conventional doxorubicin for first-line treatment of metastatic breast cancer. *Ann. Oncol* 15, 440–449 [PubMed: 14998846]
43. Löfblom J et al. (2010) Affibody molecules: engineered proteins for therapeutic, diagnostic and biotechnological applications. *FEBS Lett.* 584, 2670–2680. 10.1016/j.febslet.2010.04.014 [PubMed: 20388508]
44. Ståhl S et al. (2017) Affibody molecules in biotechnological and medical applications. *Trends Biotechnol.* 35, 691–712. 10.1016/j.tibtech.2017.04.007 [PubMed: 28514998]
45. Kuriakose A et al. (2016) Immunogenicity of biotherapeutics: causes and association with posttranslational modifications. *J. Immunol. Res* 2016 10.1155/2016/1298473
46. Honarvar H et al. (2016) Feasibility of affibody molecule-based PNA-mediated radionuclide pretargeting of malignant tumors. *Theranostics* 6, 93–103. 10.7150/thno.12766 [PubMed: 26722376]
47. Rosestedt M et al. (2015) Affibody-mediated PET. imaging of HER3 expression in malignant tumours. *Sci. Rep* 5 10.1038/srep15226
48. Upreti M et al. (2013) Tumor microenvironment and nanotherapeutics. *Transl. Cancer Res.* 2, 309–319. 10.3978/j.issn.2218-676X.2013.08.11 [PubMed: 24634853]
49. Mansour AM et al. (2003) A new approach for the treatment of malignant melanoma: enhanced antitumor efficacy of an albumin-binding doxorubicin prodrug that is cleaved by matrix metalloproteinase 2. *Cancer Res.* 63, 4062–4066 [PubMed: 12874007]
50. Sneider A et al. (2017) Remotely triggered nano-theranostics for cancer applications. *Nanotheranostics* 1, 1–22. 10.7150/ntno.17109 [PubMed: 28191450]
51. Reddy TL et al. (2016) Simultaneous delivery of Paclitaxel and Bcl-2 siRNA via pH-sensitive liposomal nanocarrier for the synergistic treatment of melanoma. *Sci. Rep* 6, 35223 10.1038/srep35223 [PubMed: 27786239]

52. Fan Z et al. (2017) pH-Responsive fluorescent graphene quantum dots for fluorescence-guided cancer surgery and diagnosis. *Nanoscale* 9, 4928–4933. 10.1039/c7nr00888k [PubMed: 28368056]
53. Lin Y et al. (2018) Redox/ATP switchable theranostic nanoparticles for real-time fluorescence monitoring of doxorubicin delivery. *J. Mater. Chem. B* 6, 2089–2103. 10.1039/C7TB03325G
54. Tatiparti K et al. (2018) Copper-free ‘click’ chemistry-based synthesis and characterization of carbonic anhydrase-IX anchored albumin-paclitaxel nanoparticles for targeting tumor hypoxia. *Int. J. Mol. Sci* 19, 838 10.3390/ijms19030838
55. Nie S (2010) Understanding and overcoming major barriers in cancer nanomedicine. *North* 5, 523–528. 10.3174/ajnr.A1256.Functional
56. Moghimi SM and Szebeni J (2003) Stealth liposomes and long circulating nanoparticles: critical issues in pharmacokinetics, opsonization and protein-binding properties. *Prog. Lipid Res.* 42, 463–478. 10.1016/S0163-7827(03)00033-X [PubMed: 14559067]
57. Brannon-Peppas L and Blanchette JO (2012) Nanoparticle and targeted systems for cancer therapy. *Adv. Drug Deliv. Rev* 64, 206–212. 10.1016/j.addr.2012.09.033
58. Barenholz Y (2012) Doxil® — the first FDA-approved nano-drug: lessons learned. *J. Control. Release* 160, 117–134. 10.1016/j.jconrel.2012.03.020 [PubMed: 22484195]
59. Boucher Y and Jain RK (1992) Microvascular pressure is the principal driving force for interstitial hypertension in solid tumors: implications for vascular collapse. *Cancer Res.* 52, 5110–5114 [PubMed: 1516068]
60. Jain RK and Stylianopoulos T (2010) Delivering nanomedicine to solid tumors. *Nat. Rev. Clin. Oncol* 7, 653–664. 10.1038/nrclinonc.2010.139 [PubMed: 20838415]
61. Jacobetz MA et al. (2013) Hyaluronan impairs vascular function and drug delivery in a mouse model of pancreatic cancer. *Gut* 62, 112–120. 10.1136/gutjnl-2012-302529 [PubMed: 22466618]
62. Alberts B et al. (2002) The extracellular matrix of animals. *Mol. Biol. Cell* i, 1–25
63. Johnsen KB et al. (2017) Targeting transferrin receptors at the blood–brain barrier improves the uptake of immunoliposomes and subsequent cargo transport into the brain parenchyma. *Sci. Rep* 7, 1–13. 10.1038/s41598-017-11220-1 [PubMed: 28127051]
64. Menon GK et al. (2012) The structure and function of the stratum corneum. *Int. J. Pharm* 435, 3–9. 10.1016/j.ijpharm.2012.06.005 [PubMed: 22705878]
65. van Smeden J and Bouwstra JA (2016) Stratum corneum lipids: their role for the skin barrier function in healthy subjects and atopic dermatitis patients. *Curr. Probl. Dermatol* 49, 8–26. 10.1159/000441540 [PubMed: 26844894]
66. Alkilani AZ et al. (2015) Transdermal drug delivery: Innovative pharmaceutical developments based on disruption of the barrier properties of the stratum corneum. *Pharmaceutics* 7, 438–470. 10.3390/pharmaceutics7040438 [PubMed: 26506371]
67. Giubudagian M et al. (2018) Breaking the barrier — potent anti-inflammatory activity following efficient topical delivery of etanercept using thermoresponsive nanogels. *Theranostics* 8, 450–463. 10.7150/thno.21668 [PubMed: 29290820]
68. Prausnitz MR and Langer R (2009) Transdermal drug delivery. *Nat. Biotechnol* 26, 1261–1268. 10.1038/nbt.1504.Transdermal
69. Lin M-W et al. (2016) A formulation study of 5-aminolevulinic acid encapsulated in DPPC liposomes in melanoma treatment. *Int. J. Med. Sci* 13, 483–489. 10.7150/ijms.15411 [PubMed: 27429584]
70. Dianzani C et al. (2014) Drug delivery nanoparticles in skin cancers. *Biomed. Res. Int* 2014 10.1155/2014/895986
71. Muhamad II and Selvakumaran S (2014) Designing polymeric nanoparticles for targeted drug delivery system outline In *Nanomedicine Book*. 287–313 Chapter 11, 12 (n.d.)
72. Wurm FR and Weiss CK (2014) Nanoparticles from renewable polymers. *Nanomedicine* 2, 287–313. 10.3389/fchem.2014.00049 (Chapter 11)
73. Elzoghby AO et al. (2016) Natural polymeric nanoparticles for brain-targeting: implications on drug and gene delivery. *Curr. Pharm. Des* 22, 3305–3323. 10.2174/1381612822666160204120829 [PubMed: 26845323]
74. Anwunobi AP and Emeje MO (2011) Recent applications of natural polymers in nanodrug delivery. *J. Nanomed. Nanotechnol* s4 10.4172/2157-7439.S4-002

75. Gültekin HE et al. (2013) Biodegradable polymeric nanoparticles are effective systems for controlled drug delivery. *J. Pharm. Sci* 38, 107–118
76. Makadia HK and Siegel SJ (2011) Poly lactic-co-glycolic acid (PLGA) as biodegradable controlled drug delivery carrier. *Polymers (Basel)* 3, 1377–1397. 10.3390/polym3031377 [PubMed: 22577513]
77. Loos C et al. (2014) Functionalized polystyrene nanoparticles as a platform for studying bio-nano interactions. *Beilstein J. Nanotechnol* 5, 2403–2412. 10.3762/bjnano.5.250 [PubMed: 25671136]
78. Dhandayuthapani B et al. (2011) Polymeric scaffolds in tissue engineering application: a review. *Int. J. Polym. Sci* 2011, 1–19. 10.1155/2011/290602
79. Kesharwani P and Iyer AK (2015) Recent advances in dendrimer-based nanovectors for tumor-targeted drug and gene delivery. *Drug Discov. Today* 20, 536–547. 10.1016/j.drudis.2014.12.012 [PubMed: 25555748]
80. Alexis F et al. (2008) Factors affecting the clearance and biodistribution of polymeric nanoparticles. *Mol. Pharm* 5, 505–515. 10.1021/mp800051m [PubMed: 18672949]
81. Sahu P et al. (2017) pp. 6–8
82. Gawde KA et al. (2017) Synthesis and characterization of folate decorated albumin bio-conjugate nanoparticles loaded with a synthetic curcumin difluorinated analogue. *J. Colloid Interface Sci.* 496, 290–299 [PubMed: 28236692]
83. Duncan R (2003) The dawning era of polymer therapeutics. *Nat. Rev. Drug Discov.* 2, 347–360. 10.1038/nrd1088 [PubMed: 12750738]
84. Tatiparti K et al. (2017) siRNA delivery strategies: a comprehensive review of recent developments. *Nanomaterials* 7, 77 10.3390/nano7040077
85. Crucho CIC and Barros MT (2017) Polymeric nanoparticles: a study on the preparation variables and characterization methods. *Mater. Sci. Eng C* 80, 771–784. 10.1016/j.msec.2017.06.004
86. Li J et al. (2015) Polymeric drugs: advances in the development of pharmacologically active polymers. *J. Control. Release* 219, 369–382. 10.1016/j.jconrel.2015.09.043 [PubMed: 26410809]
87. Masood F (2016) Polymeric nanoparticles for targeted drug delivery system for cancer therapy. *Mater. Sci. Eng C* 60, 569–578. 10.1016/j.msec.2015.11.067
88. Matsumura Y and Maeda HA (1986) A new concept for macromolecular therapeutics in cancer-chemotherapy — mechanism of tumorotropic accumulation of proteins and the antitumor agent smancs. *Cancer Res.* 46, 6387–6392 [PubMed: 2946403]
89. Ding G-B et al. (2017) A novel doxorubicin prodrug with GRP78 recognition and nucleus-targeting ability for safe and effective cancer therapy. *Mol. Pharm* 15 (1), 238–246. 10.1021/acs.molpharmaceut.7b00830 [PubMed: 29207873]
90. Jawahar N and Meyyanathan S (2012) Polymeric nanoparticles for drug delivery and targeting: a comprehensive review. *Int. J. Health Allied Sci.* 1, 217 10.4103/2278-344X.107832
91. LoPresti C et al. (2009) Polymersomes nature inspired nanometer sized compartments. *J. Mater. Chem* 19, 3576 10.1039/b818869f
92. Daglar B et al. (2014) Polymeric nanocarriers for expected nanomedicine: current challenges and future prospects. *RSC Adv.* 4, 48639–48659. 10.1039/C4RA06406B
93. Kocak G et al. (2017) pH-Responsive polymers. *Polym. Chem* 8, 144–176. 10.1039/C6PY01872F
94. Wang Q et al. (2017) Core shell lipid-polymer hybrid nanoparticles with combined docetaxel and molecular targeted therapy for the treatment of metastatic prostate cancer. *Sci. Rep* 7, 5901 10.1038/s41598-017-06142-x [PubMed: 28724986]
95. Zhang RX et al. (2017) Design of nanocarriers for nanoscale drug delivery to enhance cancer treatment using hybrid polymer and lipid building blocks. *Nanoscale* 9, 1334–1355. 10.1039/C6NR08486A [PubMed: 27973629]
96. Dumoga S et al. (2017) Block copolymer based nanoparticles for theranostic intervention of cervical cancer: synthesis pharmacokinetics, and in vitro/in vivo evaluation in HeLa xenograft models. *ACS Appl. Mater. Interfaces* 9, 22195–22211. 10.1021/acsami.7b04982 [PubMed: 28608677]
97. Jensen EC (2012) Use of fluorescent probes: their effect on cell biology and limitations. *Anat. Rec. Adv. Integr. Anat. Evol. Biol* 295, 2031–2036. 10.1002/ar.22602

98. Greb C (2012) Fluorescent Dyes. 2012
99. Gao Z et al. (2017) A fluorescent dye with large Stokes shift and high stability: synthesis and application to live cell imaging. *RSC Adv.* 7, 7604–7609. 10.1039/C6RA27547H
100. Pal SL et al. (2011) Nanoparticle: an overview of preparation and characterization. *J. Appl. Pharm. Sci* 1, 228–234. 10.7897/2230-8407.04408
101. Sanoj Rejinold N et al. (2011) Curcumin-loaded biocompatible thermoresponsive polymeric nanoparticles for cancer drug delivery. *J. Colloid Interface Sci.* 360, 39–51. 10.1016/J.JCIS.2011.04.006 [PubMed: 21549390]
102. Motlagh NSH et al. (2016) Fluorescence properties of several chemotherapy drugs: doxorubicin, paclitaxel and bleomycin. *Biomed. Opt. Express* 7, 2400–2406. 10.1364/BOE.7.002400 [PubMed: 27375954]
103. Bahmani B et al. (2014) Functionalized polymeric nanoparticles loaded with indocyanine green as theranostic materials for targeted molecular near infrared fluorescence imaging and photothermal destruction of ovarian cancer cells. *Lasers Surg. Med* 46, 582–592. 10.1002/lsm.22269 [PubMed: 24961210]
104. Chatterjee M et al. (2017) A novel approach to fabricate dye-encapsulated polymeric micro- and nanoparticles by thin film dewetting technique. *J. Colloid Interface Sci.* 506, 126–134. 10.1016/J.JCIS.2017.07.023 [PubMed: 28732229]
105. Laskar P et al. (2014) In vitro evaluation of pH-sensitive cholesterol-containing stable polymeric micelles for delivery of camptothecin. *J. Colloid Interface Sci.* 430, 305–314. 10.1016/J.JCIS.2014.05.068 [PubMed: 24974243]
106. Zhou Z et al. (2017) Sequential delivery of erlotinib and doxorubicin for enhanced triple negative breast cancer treatment using polymeric nanoparticle. *Int. J. Pharm* 530, 300–307. 10.1016/J.IJPHARM.2017.07.085 [PubMed: 28778627]
107. Wang Z et al. (2018) CD44 directed nanomicellar payload delivery platform for selective anticancer effect and tumor specific imaging of triple negative breast cancer. *Nanomedicine* 14, 1441–1454. 10.1016/j.nano.2018.04.004 [PubMed: 29678787]
108. Mohammadi M et al. (2017) Biocompatible polymersomes-based cancer theranostics: towards multifunctional nanomedicine. *Int. J. Pharm* 519, 287–303. 10.1016/j.ijpharm.2017.01.037 [PubMed: 28115259]
109. Messenger L et al. (2014) Novel aspects of encapsulation and delivery using polymersomes. *Curr. Opin. Pharmacol* 18, 104–111. 10.1016/j.coph.2014.09.017 [PubMed: 25306248]
110. Kulkarni PS et al. (2016) Mitochondria-targeted fluorescent polymersomes for drug delivery to cancer cells. *Polym. Chem* 7, 4151–4154. 10.1039/C6PY00623J [PubMed: 27833665]
111. Pang Z et al. (2010) Lactoferrin-conjugated biodegradable polymersome holding doxorubicin and tetrandrine for chemotherapy of glioma rats. *Mol. Pharm* 7, 1995–2005. 10.1021/mp100277h [PubMed: 20957995]
112. Kulkarni P et al. (2016) Hypoxia-responsive polymersomes for drug delivery to hypoxic pancreatic cancer cells. *Biomacromolecules* 17, 2507–2513. 10.1021/acs.biomac.6b00350 [PubMed: 27303825]
113. Iyer AK et al. (2007) High-loading nanosized micelles of copoly(styrene-maleic acid)-zinc protoporphyrin for targeted delivery of a potent heme oxygenase inhibitor. *Biomaterials* 28, 1871–1881. 10.1016/j.biomaterials.2006.11.051 [PubMed: 17208294]
114. Kumar R et al. (2012) In vitro evaluation of theranostic polymeric micelles for imaging and drug delivery in cancer. *Theranostics* 2, 714–722. 10.7150/thno.3927 [PubMed: 22896773]
115. Grünwald GK et al. (2013) EGFR-targeted adenovirus dendrimer coating for improved systemic delivery of the theranostic NIS gene. *Mol. Ther. Nucleic Acids* 2 10.1038/mtna.2013.58
116. Harrington KJ et al. (2001) Effective targeting of solid tumors in patients with locally advanced cancers by radiolabeled pegylated liposomes. *Clin. Cancer Res.* 7, 243–254 [PubMed: 11234875]
117. Xu H-L et al. (2016) Glioma-targeted superparamagnetic iron oxide nanoparticles as drug-carrying vehicles for theranostic effects. *Nanoscale* 8, 14222–14236. 10.1039/C6NR02448C [PubMed: 27396404]

118. Luong D et al. (2017) Folic acid conjugated polymeric micelles loaded with a curcumin difluorinated analog for targeting cervical and ovarian cancers. *Colloids Surf. B Biointerfaces* 157, 490–502 [PubMed: 28658642]
119. Sharma H et al. (2015) Metal nanoparticles: a theranostic nanotool against cancer. *Drug Discov. Today* 20, 1143–1151. 10.1016/j.drudis.2015.05.009 [PubMed: 26007605]
120. Dolina JS et al. (2013) Lipidoid nanoparticles containing PD-L1 siRNA delivered in vivo enter kupffer cells and enhance NK and CD8(+) T cell-mediated hepatic antiviral immunity. *Mol. Ther. Nucleic Acids* 2, e72 10.1038/mtna.2012.63 [PubMed: 23423360]
121. Yang R-M et al. (2016) Hyaluronan-modified superparamagnetic iron oxide nanoparticles for bimodal breast cancer imaging and photothermal therapy. *Int. J. Nanomed* 12, 197–206. 10.2147/IJN.S121249
122. Huang Y et al. (2017) Superparamagnetic iron oxide nanoparticles conjugated with folic acid for dual target-specific drug delivery and MRI in cancer theranostics. *Mater. Sci. Eng C* 70, 763–771. 10.1016/j.msec.2016.09.052
123. Neesse A et al. (2015) Stromal biology and therapy in pancreatic cancer: a changing paradigm. *Gut* 64, 1476–1484. 10.1136/gutjnl-2015-309304 [PubMed: 25994217]
124. Lee GY et al. (2013) Theranostic nanoparticles with controlled release of gemcitabine for targeted therapy and MRI of pancreatic cancer. *ACS Nano* 7, 2078–2089. 10.1021/nn3043463 [PubMed: 23402593]
125. Bhise K et al. (2017) Nanostructured lipid carriers employing polyphenols as promising anticancer agents: quality by design (QbD) approach. *Therapeutic Delivery* 8 10.4155/tde-2017-0062
126. Liang J et al. (2017) Lipid-coated iron oxide nanoparticles for dual-modal imaging of hepatocellular carcinoma. *Int. J. Nanomed* 12, 2033–2044. 10.2147/IJN.S128525
127. Bain J et al. (2015) In situ formation of magnetopolymersomes via electroporation for MRI. *Sci. Rep* 5, 14311 10.1038/srep14311 [PubMed: 26391797]
128. Sau S et al. (2017) Combination of cationic dexamethasone derivative and STAT3 inhibitor (WP1066) for aggressive melanoma: a strategy for repurposing a phase I clinical trial drug. *Mol. Cell. Biochem* 1–18
129. Alberti D et al. (2017) Theranostic nanoparticles loaded with imaging probes and rubrocurcumin for combined cancer therapy by folate receptor targeting. *ChemMedChem* 12, 502–509. 10.1002/cmdc.201700039 [PubMed: 28217982]
130. Kumar S et al. (2017) PEG coated and doxorubicin loaded multimodal Gadolinium oxide nanoparticles for simultaneous drug delivery and imaging applications. *Int. J. Pharm* 527, 142–150. 10.1016/J.IJPHARM.2017.05.027 [PubMed: 28506803]
131. Ortega AL et al. (2011) Glutathione in cancer cell death. *Cancers (Basel)* 3, 1285–1310. 10.3390/cancers3011285 [PubMed: 24212662]
132. Zhao J et al. (2017) Redox-sensitive nanoscale coordination polymers for drug delivery and cancer theranostics. *ACS Appl. Mater. Interfaces* 9, 23555–23563. 10.1021/acsami.7b07535 [PubMed: 28636308]
133. Fanizza E et al. (2016) Fabrication of photoactive heterostructures based on quantum dots decorated with Au nanoparticles. *Sci. Technol. Adv. Mater* 17, 98–108. 10.1080/14686996.2016.1153939 [PubMed: 27877861]
134. Wen S et al. (2013) Multifunctional dendrimer-entrapped gold nanoparticles for dual mode CT/MR imaging applications. *Biomaterials* 34, 1570–1580. 10.1016/J.BIOMATERIALS.2012.11.010 [PubMed: 23199745]
135. Vyas SS and Patravale VB (2015) Advances in nanomaterials for diagnosis and therapy of leukemia. *Nanomedicine* 3, 99–104. 10.2174/1877912304666140201000322
136. Reuveni T et al. (2011) Targeted gold nanoparticles enable molecular CT imaging of cancer: an in vivo study. *Int. J. Nanomed* 6, 2859–2864. 10.2147/IJN.S25446
137. Manju S and Sreenivasan K (2012) Gold nanoparticles generated and stabilized by water soluble curcumin–polymer conjugate: blood compatibility evaluation and targeted drug delivery onto cancer cells. *J. Colloid Interface Sci.* 368, 144–151. 10.1016/J.JCIS.2011.11.024 [PubMed: 22200330]

138. Wei D et al. (2009) The synthesis of chitosan-based silver nanoparticles and their antibacterial activity. *Carbohydr. Res* 344, 2375–2382. 10.1016/j.carres.2009.09.001 [PubMed: 19800053]
139. Boca SC et al. (2011) Chitosan-coated triangular silver nanoparticles as a novel class of biocompatible, highly effective photothermal transducers for in vitro cancer cell therapy. *Cancer Lett.* 311, 131–140. 10.1016/j.canlet.2011.06.022 [PubMed: 21840122]
140. Khodashenas, and Bahareh G (2005) Synthesis of silver nanoparticles with different shapes. *Mater. Lett* 59, 1760–1763. 10.1016/j.matlet.2005.01.061
141. Dong X et al. (2010) Synthesis of triangular silver nanoprisms by stepwise reduction of sodium borohydride and trisodium citrate. *J. Phys. Chem C* 114, 2070–2074. 10.1021/jp909964k
142. Wu C et al. (2015) Localized surface plasmon resonance of silver nanotriangles synthesized by a versatile solution reaction. *Nanoscale Res. Lett* 10 10.1186/s11671-015-1058-1
143. Kelly JM et al. (2012) Triangular silver nanoparticles: their preparation, functionalisation and properties. *Acta Phys. Pol. A* 122, 337–345. 10.12693/APhysPolA.122.337
144. Mukherjee S et al. (2014) Potential theranostics application of bio-synthesized silver nanoparticles (4-in-1 system). *Theranostics* 4, 316–335. 10.7150/thno.7819 [PubMed: 24505239]
145. Sahoo AK et al. (2016) Silver nanocluster embedded composite nanoparticles for targeted prodrug delivery in cancer theranostics. *ACS Biomater. Sci. Eng* 2, 1395–1402. 10.1021/acsbiomaterials.6b00334
146. Ashenfelter BA et al. (2015) Fluorescence from molecular silver nanoparticles. *J. Phys. Chem C* 119, 20728–20734. 10.1021/acs.jpcc.5b05735
147. Qu F et al. (2013) Transition from nanoparticles to nanoclusters: Microscopic and spectroscopic investigation of size-dependent physicochemical properties of polyamine-functionalized silver nanoclusters. *J. Phys. Chem C* 117, 3548–3555. 10.1021/jp3091792
148. Yuan X et al. (2013) Highly luminescent silver nanoclusters with tunable emissions: cyclic reduction-decomposition synthesis and antimicrobial properties. *NPG Asia Mater.* 5 10.1038/am.2013.3
149. Opoku-Damoah Y et al. (2016) Versatile nanosystem-based cancer theranostics: design inspiration and predetermined routing. *Theranostics* 6, 986–1003. 10.7150/thno.14860 [PubMed: 27217832]
150. Hong H et al. (2015) Red fluorescent zinc oxide nanoparticle: a novel platform for cancer targeting. *ACS Appl. Mater. Interfaces* 7 (5), 3373–3381. 10.1021/am508440j [PubMed: 25607242]
151. Hong H et al. (2011) Cancer-targeted optical imaging with fluorescent zinc oxide nanowires. *Nano Lett.* 3744–3750 [PubMed: 21823599]
152. Crawford LV et al. (1982) Detection of antibodies against the cellular protein p53 in sera from patients with breast cancer. *Int. J. Cancer* 30, 403–408. 10.1002/ijc.2910300404 [PubMed: 6292117]
153. Vu Manh T-P and Dalod M (2016) Characterization of dendritic cell subsets through gene expression analysis. *Methods Mol. Biol* 1423, 211–243. 10.1007/978-1-4939-3606-9_16 [PubMed: 27142020]
154. Klippstein R and Pozo D (2010) Nanotechnology-based manipulation of dendritic cells for enhanced immunotherapy strategies. *Nanomedicine* 6, 523–529. 10.1016/j.nano.2010.01.001 [PubMed: 20085824]
155. Sozzani S et al. (2017) Dendritic cell recruitment and activation in autoimmunity. *J. Autoimmun* 85, 126–140. 10.1016/j.jaut.2017.07.012 [PubMed: 28774715]
156. Vanloubbeecq Y et al. (2003) The biology of dendritic cells and their potential use in veterinary medicine. *Anim. Health Res. Rev* 4, 131–142. 10.1079/AHR200354 [PubMed: 15134295]
157. Strioga M et al. (2013) Dendritic cells and their role in tumor immunosurveillance. *Innate Immun.* 19, 98–111. 10.1177/1753425912449549 [PubMed: 22732734]
158. Sabado RL et al. (2017) Dendritic cell-based immunotherapy. *Cell Res.* 27, 74–95. 10.1038/cr.2016.157 [PubMed: 28025976]
159. Böttcher JP et al. (2015) Functional classification of memory CD8+ T cells by CX3CR1 expression. *Nat. Commun* 6, 8306 10.1038/ncomms9306 [PubMed: 26404698]

160. Mahic M et al. (2008) Differentiation of naive CD4+ T cells into CD4+CD25 +FOXP3+ regulatory T cells by continuous antigen stimulation. *J. Leukoc. Biol* 83, 1111–1117. 10.1189/jlb.0507329 [PubMed: 18270250]
161. De Rezende LCD et al. (2010) Cell as a target for cancer therapy. *Arch. Immunol. Ther. Exp. (Warsz)* 58, 179–190. 10.1007/s00005-010-0075-0 [PubMed: 20373146]
162. Alsaab HO et al. (2017) PD-1 and PD-L1 checkpoint signaling inhibition for cancer immunotherapy: mechanism, combinations, and clinical outcome. *Front. Pharmacol* 8, 561 10.3389/fphar.2017.00561 [PubMed: 28878676]
163. Xiang J et al. (2015) Antigen-loaded upconversion nanoparticles for dendritic cell stimulation tracking, and vaccination in dendritic cell-based immunotherapy. *ACS Nano* 9, 6401–6411. 10.1021/acsnano.5b02014 [PubMed: 26028363]
164. Cho NH et al. (2011) A multifunctional core-shell nanoparticle for dendritic cell-based cancer immunotherapy. *Nat. Nanotechnol* 6, 675–682. 10.1038/nnano.2011.149 [PubMed: 21909083]
165. Liu Y et al. (2016) Theranostic near-infrared fluorescent nanoplatform for imaging and systemic siRNA delivery to metastatic anaplastic thyroid cancer. *Proc. Natl. Acad. Sci* 113, 7750–7755. 10.1073/pnas.1605841113 [PubMed: 27342857]
166. Lee J et al. (2016) Optical imaging and gene therapy with neuroblastoma-targeting polymeric nanoparticles for potential theranostic applications. *Small* 12, 1201–1211. 10.1002/sml.201501913 [PubMed: 26573885]
167. Luo X et al. (2017) Folic acid-functionalized polyethylenimine superparamagnetic iron oxide nanoparticles as theranostic agents for magnetic resonance imaging and PD-L1 siRNA delivery for gastric cancer. *Int. J. Nanomed* 12, 5331–5343. 10.2147/IJN.S137245
168. Wu Z et al. (2017) Magnetic cationic amylose nanoparticles used to deliver survivin-small interfering RNA for gene therapy of hepatocellular carcinoma in vitro. *Nanomater (Basel, Switzerland)* 7 10.3390/nano7050110
169. Wei P et al. (2016) Dendrimer-stabilized gold nanostars as a multifunctional theranostic nanoplatform for CT imaging photothermal therapy, and gene silencing of tumors. *Adv. Healthc. Mater* 5, 3203–3213. 10.1002/adhm.201600923 [PubMed: 27901317]
170. Alberti D et al. (2017) Theranostic nanoparticles loaded with imaging probes and rubrocurcumin for combined cancer therapy by folate receptor targeting. *ChemMedChem* 12, 502–509 [PubMed: 28217982]
171. Zhao J et al. (2018) Redox-sensitive nanoscale coordination polymers for drug delivery and cancer theranostics. *ACS Appl. Mater. Interfaces* 9 (28), 23555–23563. 10.1021/acscami.7b07535 2017:acscami.7b07535
172. Bahadar H et al. (2016) Toxicity of nanoparticles and an overview of current experimental models. *Iran. Biomed. J* 20, 1–11. 10.7508/ibj.2016.01.001 [PubMed: 26286636]
173. Makadia HK and Siegel SJ (2011) Poly Lactic-co-Glycolic Acid (PLGA) as biodegradable controlled drug delivery carrier. *Polymers (Basel)* 3, 1377–1397. 10.3390/polym3031377 [PubMed: 22577513]
174. Grabowski N et al. (2015) Surface coating mediates the toxicity of polymeric nanoparticles towards human-like macrophages. *Int. J. Pharm* 482, 75–83. 10.1016/j.ijpharm.2014.11.042 [PubMed: 25448553]
175. Voigt N et al. (2014) Toxicity of polymeric nanoparticles in vivo and in vitro. *J. Nanopart. Res* 16, 1–22. 10.1007/s11051-014-2379-1
176. De Jong WH and Borm PJA (2008) Drug delivery and nanoparticles: applications and hazards. *Int. J. Nanomed* 3, 133–149. 10.2147/IJN.S596
177. Qi Y and Chilkoti A (2015) Protein-polymer conjugation-moving beyond PEGylation. *Curr. Opin. Chem. Biol* 28, 181–193. 10.1016/j.cbpa.2015.08.009 [PubMed: 26356631]
178. Richter AW and Åkerblom E (1983) Antibodies against polyethylene glycol produced in animals by immunization with monomethoxy polyethylene glycol modified proteins. *Int. Arch. Allergy Immunol.* 70, 124–131. 10.1159/000233309
179. Dewachter P and Mouton-Faivre C (2005) Anaphylaxis to macrogol 4000 after a parenteral corticoid injection. *Allergy Eur. J. Allergy Clin. Immunol* 60, 705–706. 10.1111/j.1398-9995.2005.00783.x

180. Armstrong JK et al. (2007) Antibody against poly(ethylene glycol) adversely affects PEG-asparaginase therapy in acute lymphoblastic leukemia patients. *Cancer* 110, 103–111. 10.1002/cncr.22739 [PubMed: 17516438]
181. Mondini S et al. (2015) Zwitterion-coated iron oxide nanoparticles: surface chemistry and intracellular uptake by hepatocarcinoma (HepG2) cells. *Langmuir* 31, 7381–7390. 10.1021/acs.langmuir.5b01496 [PubMed: 26057696]
182. Liu S and Jiang S (2016) Zwitterionic polymer-protein conjugates reduce polymer-specific antibody response. *Nano Today* 11, 285–291. 10.1016/j.nantod.2016.05.006
183. Naqvi S et al. (2010) Concentration-dependent toxicity of iron oxide nanoparticles mediated by increased oxidative stress. *Int. J. Nanomed* 5, 983–989. 10.2147/IJN.S13244
184. Mahmoudi M et al. (2012) Assessing the in vitro and in vivo toxicity of superparamagnetic iron oxide nanoparticles. *Chem. Rev* 112, 2323–2338. 10.1021/cr2002596 [PubMed: 22216932]
185. Singh N et al. (2010) Potential toxicity of superparamagnetic iron oxide nanoparticles (SPION). *Nano Rev.* 1, 5358 10.3402/nano.v1i0.5358
186. Alkilany AM and Murphy CJ (2010) Toxicity and cellular uptake of gold nanoparticles: what we have learned so far? *J. Nanopart. Res* 12, 2313–2333. 10.1007/s11051-010-9911-8 [PubMed: 21170131]
187. Osman IF et al. (2010) Genotoxicity and cytotoxicity of zinc oxide and titanium dioxide in HEp-2 cells. *Nanomedicine* 5, 1193–1203. 10.2217/nnm.10.52 [PubMed: 21039197]
188. Zaitseva NV et al. (2015) Acute inhalation toxicity of manganese oxide nanoparticles. *Nanotechnol. Russ* 10, 468–474. 10.1134/S1995078015030180
189. Dvořáková M et al. (2017) Effect of neonatal exposure to poly(ethylene glycol)-block-poly(lactic acid) nanoparticles on oxidative state in infantile and adult female rats. *Oxid. Med. Cell. Longev* 2017, 1–8. 10.1155/2017/7430435
190. Noori A et al. (2013) Effect of magnetic iron oxide nanoparticles on pregnancy and testicular development of mice. *Afr. J. Biotechnol* 10, 1221–1227. 10.5897/AJB10.1544
191. Zhu X et al. (2012) Toxicity assessment of iron oxide nanoparticles in zebrafish (*Danio rerio*) early life stages. *PLoS One* 7 10.1371/journal.pone.0046286
192. Zhu MT et al. (2008) Comparative study of pulmonary responses to nano- and submicron-sized ferric oxide in rats. *Toxicology* 247, 102–111. 10.1016/j.tox.2008.02.011 [PubMed: 18394769]
193. Sung JH et al. (2008) Lung function changes in Sprague–Dawley rats after prolonged inhalation exposure to silver nanoparticles. *Inhal. Toxicol* 20, 567–574. 10.1080/08958370701874671 [PubMed: 18444009]
194. Siddiqi NJ et al. (2012) Identification of potential biomarkers of gold nanoparticle toxicity in rat brains. *J. Neuroinflammation* 9, 656 10.1186/1742-2094-9-123
195. Abbasalipourkabir R et al. (2015) Toxicity of zinc oxide nanoparticles on adult male Wistar rats. *Food Chem. Toxicol* 84, 154–160. 10.1016/j.fct.2015.08.019 [PubMed: 26316185]
196. Multimodal, Multifunctional Polymer Coated Nanoparticles. 2009
197. Magnetic Nanoplatforams for Theranostic and Multi-Modal Imaging Applications. 2011
198. Polymeric Systems and Uses Thereof in Theranostic Applications. 2015
199. Novel Theranostic Platform for Targeted Cancer Therapy and Drug Delivery Monitoring. 2013
200. Nir Materials and Nanomaterials for Theranostic Applications. 2011
201. Polymer Nanocapsules Entrapping Metal Nanoparticles. 2011
202. Tumour-Targeted Theranostic. 2014
203. Fluorescent Magnetic Nanoparticles and Process of Preparation. 2003
204. Magnetic Nanoparticles Linked to a Ligand. 2004
205. Karkada M et al. (2014) Therapeutic vaccines and cancer: focus on DPX-0907. *Biologics* 8, 27–38. 10.2147/BTT.S55196 [PubMed: 24596453]

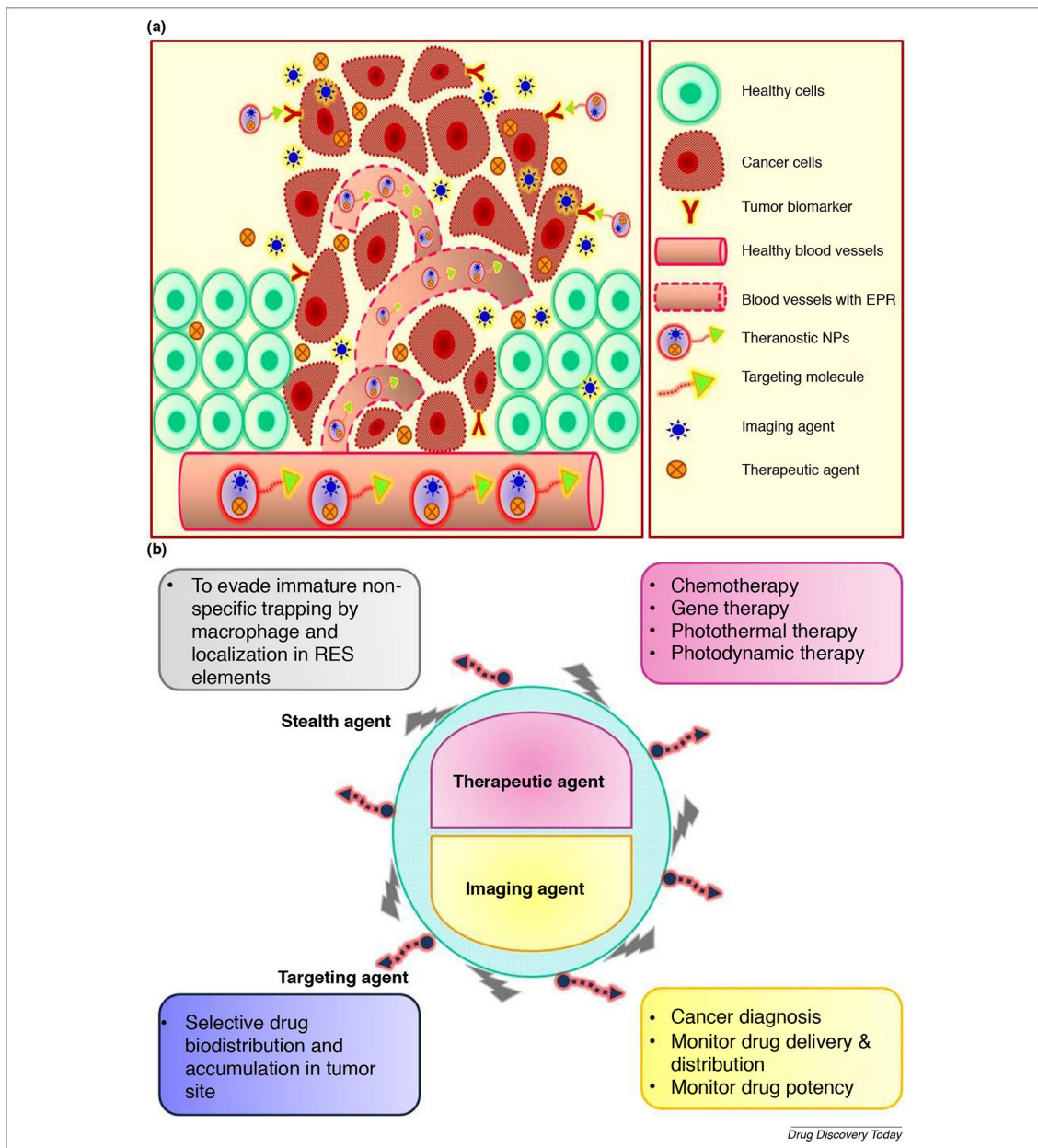


FIGURE 1. (a) Active and passive tumor targeting with theranostic NPs. (b) Demonstration of the versatile characteristics of the theranostic NPs.

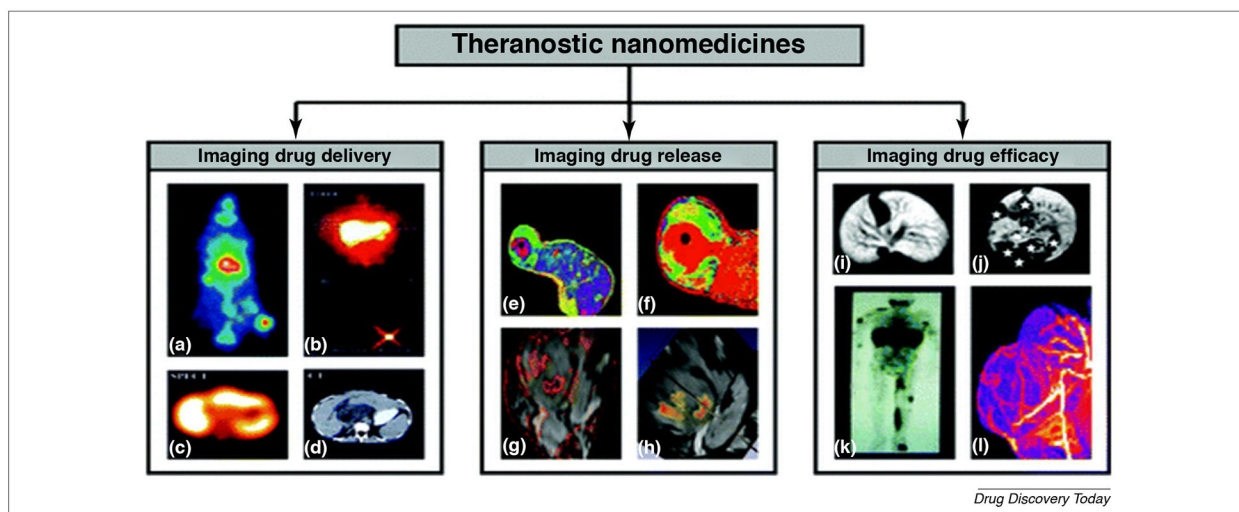


FIGURE 2.

Theranostic drug delivery system (DDS): is a new non-invasive imaging technique to check the ability of the pharmaceutical formulation to deliver the drug (**a–d**), to control drug release (**e–h**) and to determine the impact of this formulation on the drug efficacy (**i–l**). (**a**) EPR induced accumulation of iodine –131 labeled HPMA copolymer in the Dunning AT1 animal model.

(**b–d**) Different imaging modalities such as gamma camera, SPECT, and CT are used to monitor the delivery of galactosamine targeted HPMA copolymer containing DOX and labeled with iodine –123 to liver cancer.

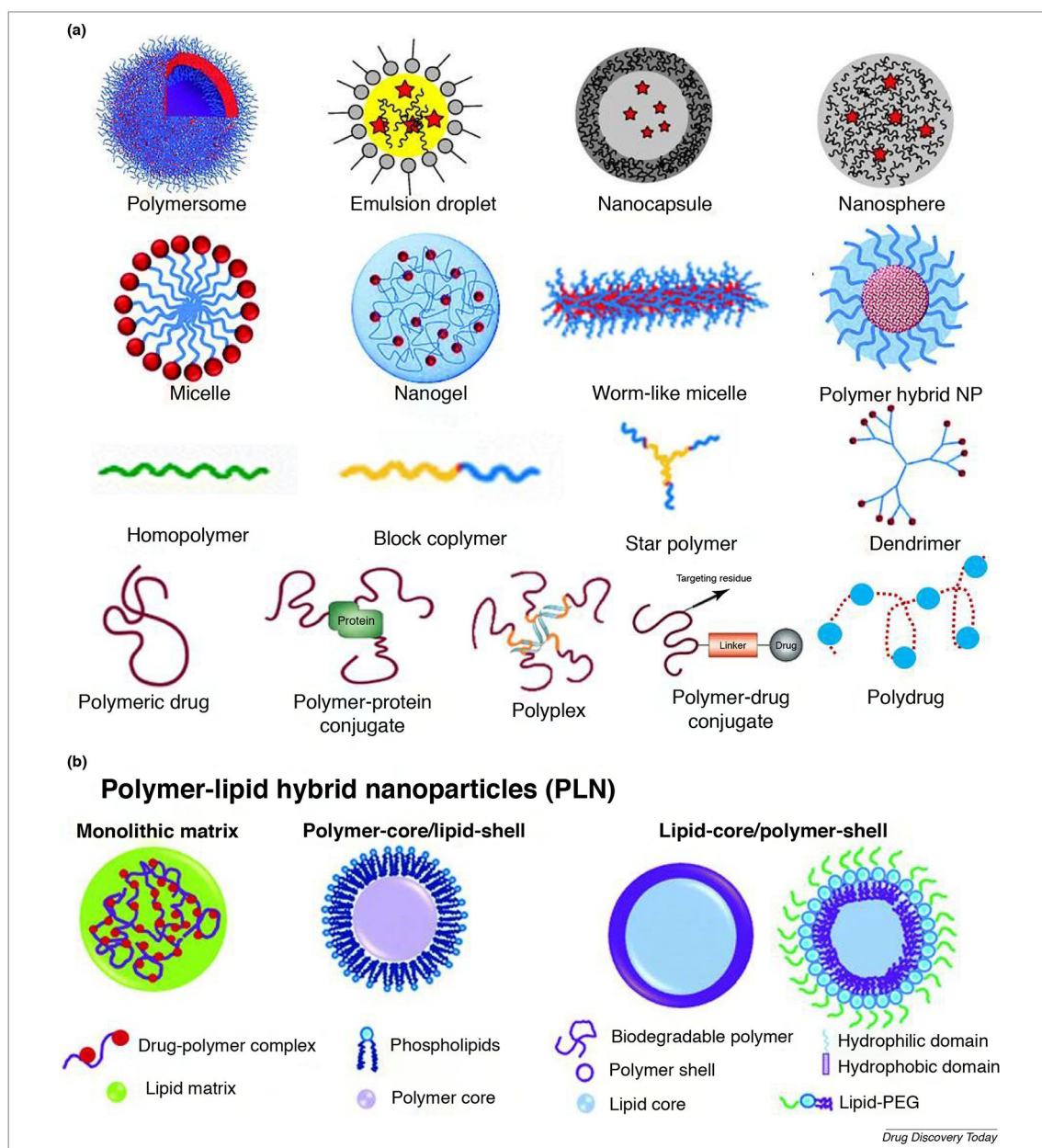
(**e** and **f**) MR was used as a tool to determine the percent of released DOX from the temperature-sensitive liposome (TSL) encapsulating both manganese as MRI contrasting agent and DOX as a therapeutic agent.

(**g** and **h**) PLGA nanoparticle with Gd-DTPA, SPIO, and 5-FU core was used to create multiple contrasting signals in the tumor and give an idea about PLGA dissociation.

(**i** and **j**) Gd-labeled polypropylene diaminobutane dendrimers showed high affinity for liver cancer and metastatic lesions.

(**k**) Indium-111 labeled PEGylated liposomes demonstrated the ability of stealth NPs to bypass capturing by RES and accumulate in the tumor side in patients with Kaposi sarcoma.

(**l**) Gadolinium labeled HPMA copolymer showed a marked affinity and high anticancer potency in Dunning AT1 animal model. The images are adapted with permission from Ref. [35].

**FIGURE 3.**

(a) Classification of polymer NPs based on their shape; polymersome, emulsion droplet, nanocapsule, nanosphere, micelle, nanogel, worm like micelle, polymer hybrid, homopolymer, block copolymer, star polymer, dendrimer, polymeric drug [86], polymer-protein conjugate, polyplex, polymer-drug conjugate, and polydrug [86]. The images are adapted with permission [83,85,91–93]. **(b)** Different forms of polymer-lipid hybrid NPs. Polymer-lipid hybrid NPs is a robust drug delivery architecture consists of both polymer and lipid materials and takes the advantages of both polymeric and liposomal drug delivery. It is well established that liposome is biocompatible while polymers are stable with high drug encapsulating capacity. The polymer-lipid hybrid system will combine the advantages of both systems providing sustained drug release, improved bio-functionality, enhanced serum

stability with the ability to encapsulate the hydrophilic drug in polymer layer and hydrophobic drug in lipid layer [94]. The image is adapted with permission [95].

Author Manuscript

Author Manuscript

Author Manuscript

Author Manuscript

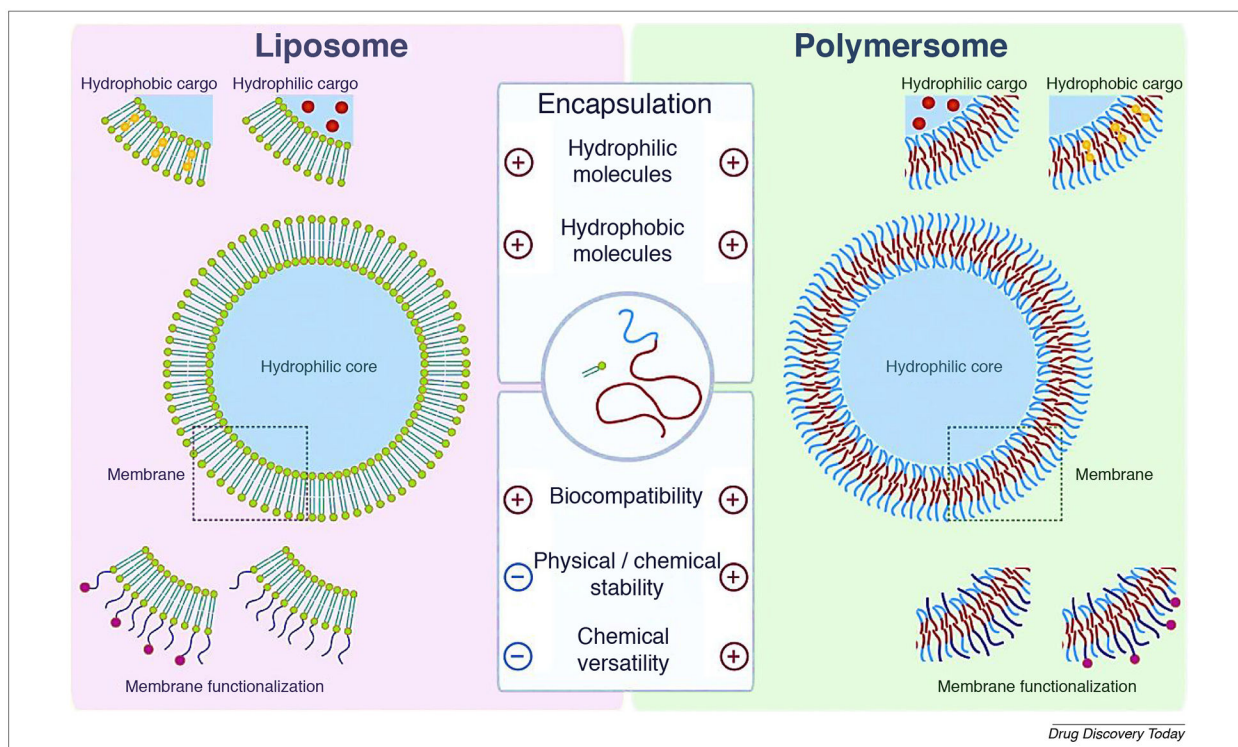


FIGURE 4.

Polymersome is emerging as a promising candidate for drug delivery possesses outperforming features than liposome. A liposome is a well-established drug delivery vesicle which consists of an aqueous core surrounded by natural bilipid membrane. The core is suitable for hydrophilic drugs while the bilipid layer is suitable for lipophilic drugs. Even there are many marketed liposome preparations; it has some limiting features such as physical and chemical stability. polymer stealth agents such as PEG are used to enhance liposome stability in the biological environment. Polymersome is a synthetic vesicle consist of an aqueous core surrounded by amphiphilic block copolymer membrane. The membrane is hydrophilic from inside and outside aspects while it is hydrophobic in the middle part. core and the two sides of the membrane is suitable for hydrophilic drugs while the middle of the membrane is suitable for hydrophobic drugs. Polymersome overcame a lot of liposomal limitations such as physical and chemical stability, stability in the biological environment. The images are adapted with permission [109].

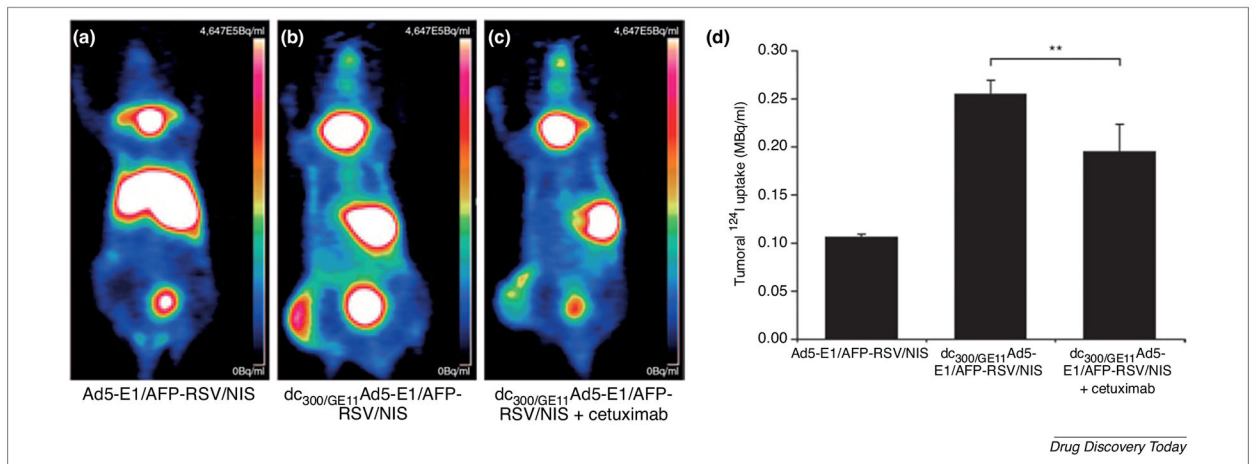


FIGURE 5.

The ¹²⁴I-PET imaging and quantitative analysis of the impact of radioiodine accumulation on gene transduction of three tested groups are presented. The injection of the plain uncoated vector (Ad5-E1/AFP-RSV/NIS) resulted in increasing liver accumulation with poor transduction ability (a and d). However, consistent liver accumulation with potent transduction ability was demonstrated by targeted coated (dc300/GE11Ad5-E1/AFP-RSV/NIS) formulation (b and d). The specificity of EGFR to liver cancer was tested by pre-injection of anti-EGFR monoclonal antibody cetuximab; The results showed a reduction in liver pooling without affecting gene transduction (c and d). (AFP) α -fetoprotein; (EGFR) epidermal growth factor receptor; and (NIS) sodium iodide symporter. The images are adapted with permission [115].

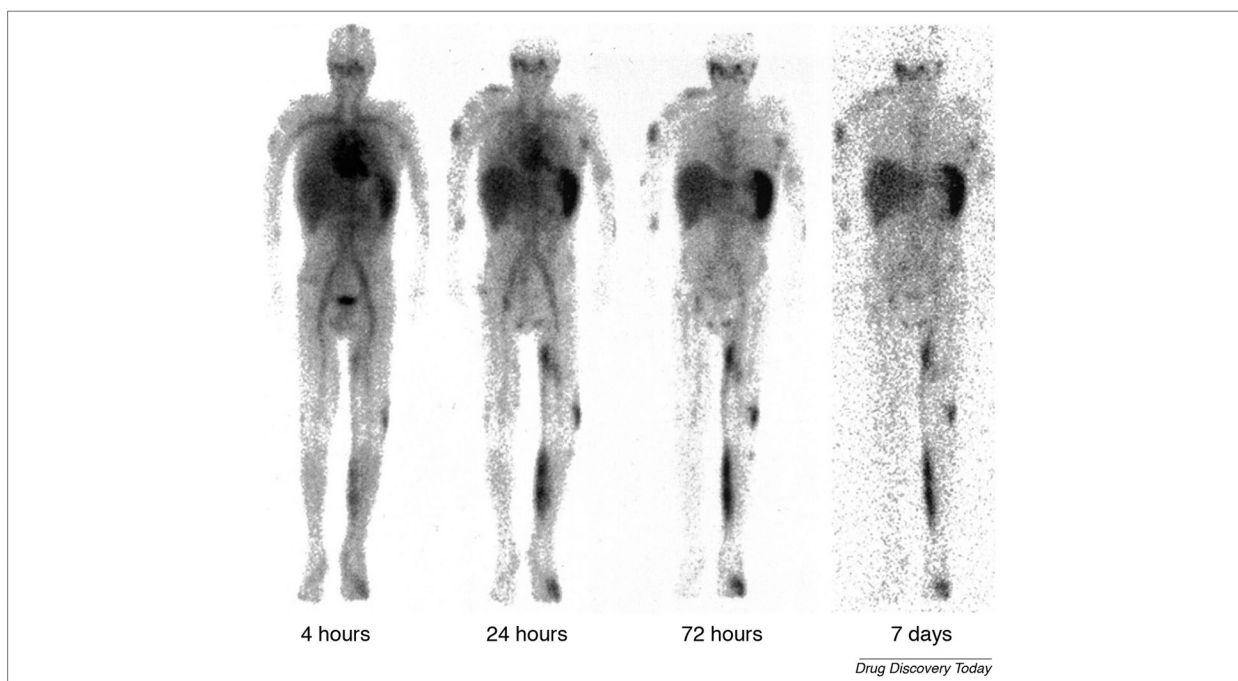


FIGURE 6.

Gamma whole body scanning of a patient with $T_1I_1S_1$ AIDS-KS in different time points 4 h, 24 h, 72 h, and seven days showed the better distribution of radiolabeled PEGylated liposome in the tumor metastatic lesions including left lower limb, right upper arm and face. The image also showed the impact of PEGylating to increase the half-life time of liposome. The images are adapted with permission from Ref. [116].

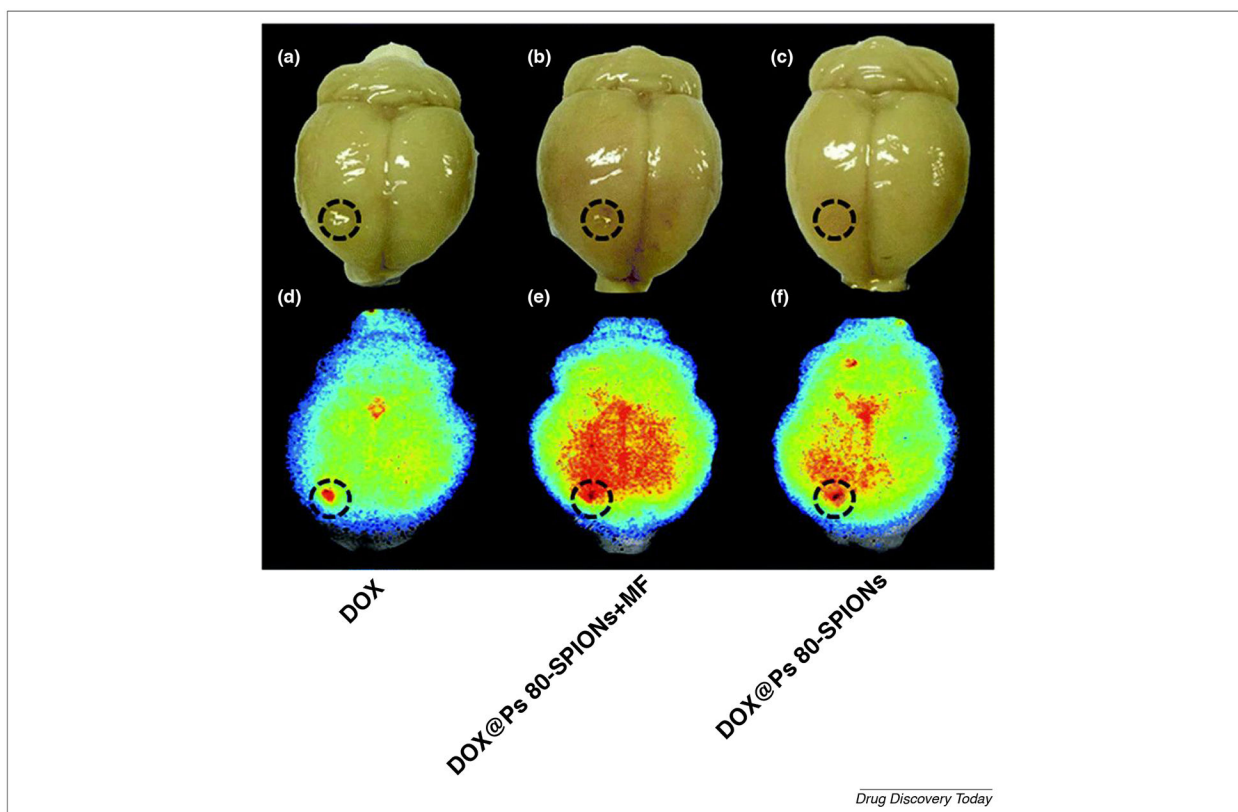


FIGURE 7.

Ex vivo comparative study carried on C6 glioma-bearing rats after two hours of administration of free Dox, DOX-Ps 80-SPIONs and DOX-Ps 80-SPIONs combined with a magnetic field. The DOX NIR fluorescent assay revealed that magnetic field improves formulation deposition in tumor site when compared to free DOX and formulation alone. The images are adapted with permission [117].

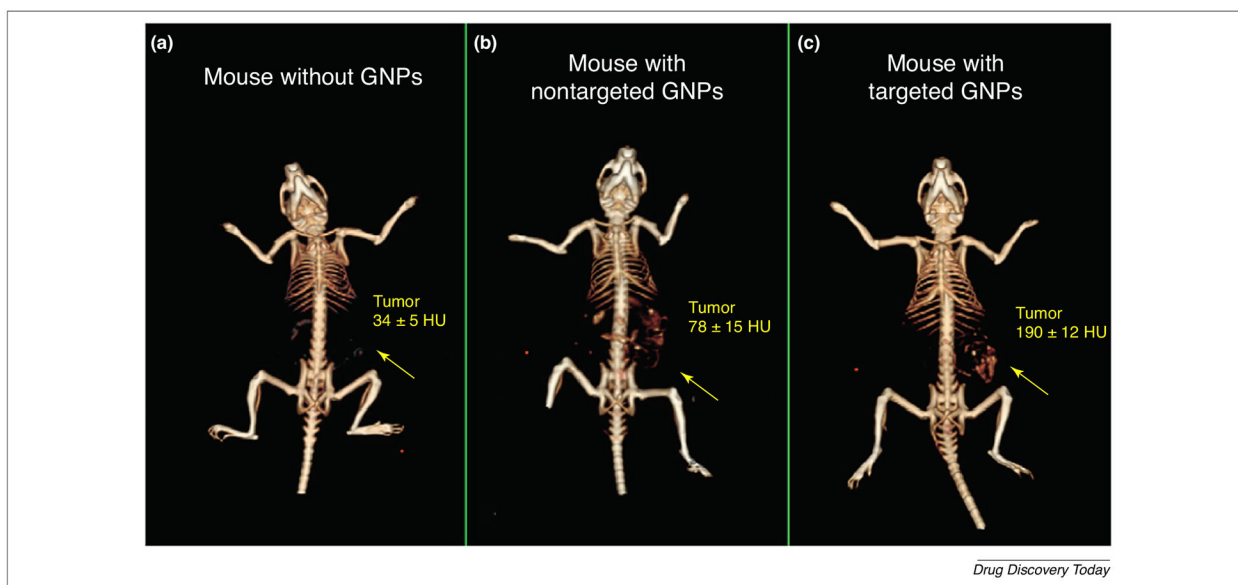
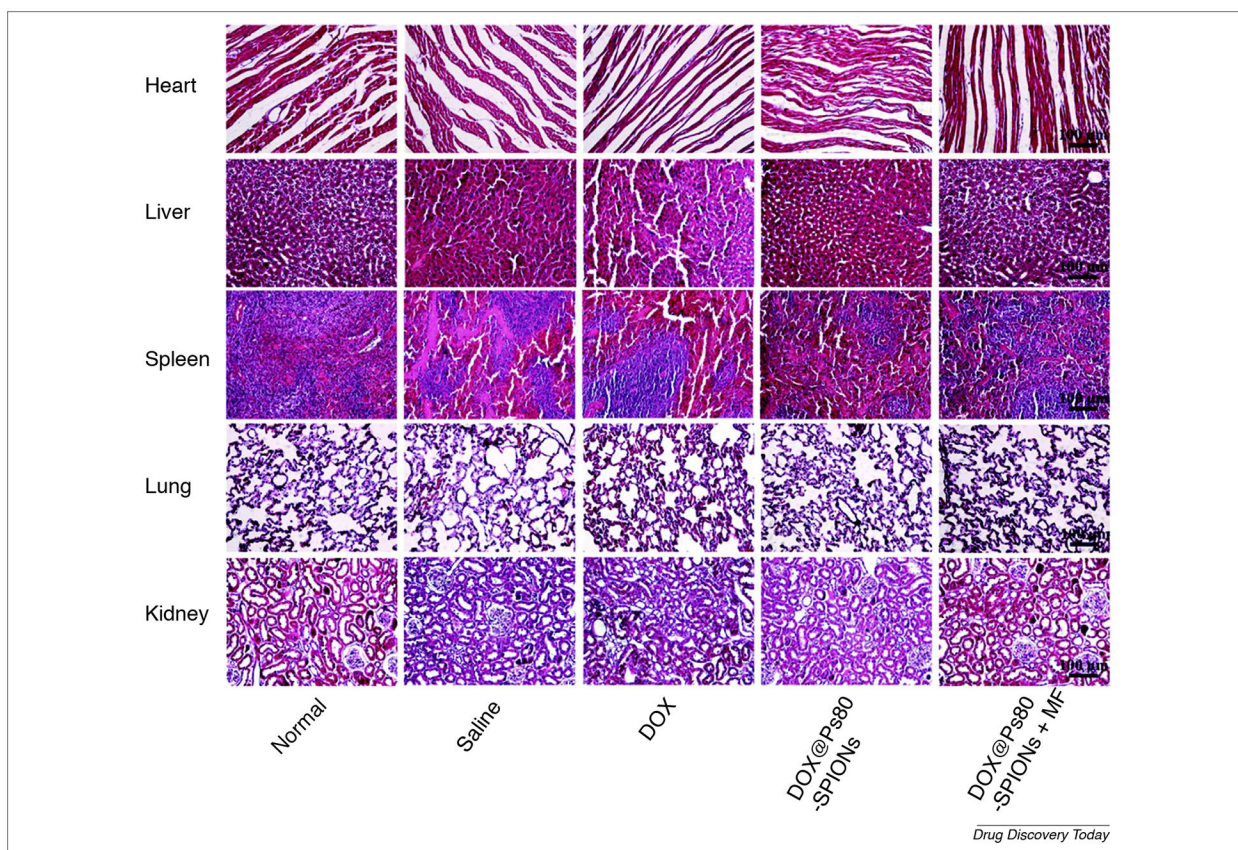


FIGURE 8.

Mice with anatomically non-detectable squamous SCC were imaged before injection (a) and 6 h after injection of both gold NPs passively targeted with anti-rabbit immunoglobulin G (b) and gold NPs actively targeted with anti-EGFR (c). The results showed enhancing tumor imaging with the actively targeted formulation with 190 ± 12 HU CT number when compared to passively targeted and non-injected animal with 78 ± 15 and 34 ± 5 HU CT number, respectively. The images are adapted with permission [136].

**FIGURE 9.**

H&E Histological sections of organs from glioma-bearing rats after being treated with saline, 6 mg kg^{-1} free DOX four times, an equivalent dose of DOX-Ps 80-SPIONs and an equivalent dose of DOX-Ps 80-SPIONs with magnetic field formulations for 28 days. The result revealed no cardiac toxicity for the encapsulated DOX when compared to free DOX. RES organs such as liver, spleen, lung, and kidney, showed minor changes for the formulation when compared to free DOX. The images are adapted with permission [117].

TABLE 1

Comparison between antibody and affibody as a targeting ligand

	Antibody	Affibody
Structure	Intact IgG monoclonal antibody	Small peptide chain
Size	Large size around 150 kDa	Small size around 6.5 kDa [43]
Affinity & specificity	Strong	Strong [43]
Heat stability	Poor	Stable
Manufacturing process	Difficult process	Easy process
Production	<i>In vivo</i> depending on the immune system	<i>In vitro</i> by chemical synthesis or by inexpensive bacterial production [44] (Originally IgG-binding, Z domain derived from <i>staphylococcal</i> surface protein A).
Cost	Costly	Not costly
Immunogenicity	The early produced murine antibodies generated human anti-mouse antibody (HAMA) response. After which the production of humanized monoclonal antibodies has been significantly decreasing the immunogenic reactions such as anaphylactic shock. However, some humanized antibodies still carry immunological risk [45]	Non-immunogenic [46]
Clearance	Long circularity time	Rapid clearance of unbound trace due to its small size [47]
Imaging properties	<ul style="list-style-type: none"> - Acceptable imaging contrast - Analysis few days after injection - Acceptable tumor penetration - Compatible with variable detection method. 	<ul style="list-style-type: none"> - Strong imaging contrast - Analysis few hours after injection - Better tumor penetration due to small size and enhanced EPR effect. - Minimal background and interference. - Compatible with variable detection method [47]
Examples	<ul style="list-style-type: none"> - Pertuzumab: anti HER2+ antibody - Ofatumumab: anti-CD20 	<ul style="list-style-type: none"> - ABY-035: anti-IL-17 - HEHEHE-Z08698-NOTA: anti-HER3 affibody

TABLE 2

Here is a summary table for the theranostic NPs extensively illustrated in the previous sections

Type of the nanosystem	Therapeutic agent	Imaging agent	Targeting ligand	Tested application	Reference
Class	Construct				
Polymer NPs	PLGA core + phospholipids & cholesterol shell Polymer-lipid hybrid	Docetaxel + FTY720	Rhodamine B & CF488	Castration-resistant prostate cancer	[94]
	Triblock copolymer (GEG) & diblock copolymer conjugate (EG)	Methotrexate (MTX)	Folic acid	Human cervical carcinoma	[96]
	Poly(allylamine) hydrochloride & PEG	Photothermal therapy (NIR laser irradiation at 808 nm)	Anti-HER2 antibody	Ovarian cancer	[103]
	PLGA	Rhodamine B		Lung cancer	[104]
	Chitosan- <i>g</i> -poly (<i>N</i> -vinylcaprolactam)	Curcumin		Prostate cancer	[101]
	PEG & cholesterol micelles	Camptothecin (CPT)		Breast & cervical cancer	[105]
	PLA- <i>b</i> -PEG	Erlotinib & doxorubicin	Coumarin 153	Breast cancer	[106]
	SMA-TPGS & HA-SMA-TPGS micelles	CDF	Rhodamine B & S0456 NIR	Breast cancer	[107]
	PLA-PEG Polymerosome	DOX	Fluorescent analogue of TPP	Pancreatic cancer	[110]
	MPEG3k-PCL 15k & HOOC-PEG 3.4k-PCL15k Polymerosome	DOX & Tet	DiR	Glioma	[111]
	PLA-azobenzene-PEG Polymerosome	Gemcitabine & erlotinib	Carboxyfluorescein dye	Pancreatic cancer	[112]
	DSPE-mPEG-2000 & DSPC Micelles	DOX	CdSe	Human cervical carcinoma	[114]
	PAMAM Dendrimer	(131)I & radiotherapy	NIS	Liver cancer	[115]
	IDLPL Stealth Liposome	¹¹¹ In-DTPA	GE11	Breast, lung, glioma, cervix, head and neck, mucocutaneous AIDS-related Kaposi sarcoma	[116]
	PEG/PEI/PS 80 Stealth SPIONs	DOX	SPIONs	Glioma	[117]
	UPP	Ovalbumin model gene	UCNPs	Dendritic cell-based immunotherapy	[163]
	Poly PCPDTBT	BRAF-siRNA	PolyPCPDTBT	ATC	[165]
	PLG	siMyc, siBcl-2, and siVEGF	FITC	Neuroblastoma	[166]
	PLGA	RbCur + Gd NCT	Gd	Ovarian cancer	[170]
	Dithiodiglycolic acid + PDA + PEG	DOX	Mn ²⁺	Breast cancer	[171]
Metal NPs	SPIONs	Photothermal NIR	SPIONs	Breast cancer	[121]
			HA		

Type of the nanosystem	Therapeutic agent	Imaging agent	Targeting ligand	Tested application	Reference
Class					
Construct					
SPIONs + PAMAM	CDF	SPIONs	FA	Ovarian & cervical cancer	[3]
SPIONs+ PEG + PEI	DOX + magnetic field	SPIONs	Folic acid	Breast cancer	[122]
IONPs	Gemcitabine	IONPs	UPA	Pancreatic cancer	[124]
SPIONs		NIR dye	Galactosamine	Liver cancer	[126]
Magnetopolymerosome	Magnetic hyperthermia	MNPs	Magnetic field		[127]
PLGA	RbCur + gadolinium/(NCT)	Gadolinium	Folate	Ovarian cancer	[129]
Gd-PEG-dox NPs	Doxorubicin	Doxorubicin & gadolinium		Lung, pancreatic & brain cancer	[130]
Mn-SS/DOX NPs + PDA + PEG	Doxorubicin	Mn ²⁺		Breast, cervical & bone cancer	[132]
Silica, gold & QDs	Gold mediated photo-thermal therapy	Gold & QDs		Glioma	[133]
Gold	Gene therapy (downregulate p-AKT).		Dexamethasone	Melanoma, Lung and breast cancer.	[14]
Gd-loaded PAMAM – entrapped gold NPs + PEG		Gd & gold		Cytocompatibility study of this NPs on Papilloma (KB cells)	[134]
Gold + PEG		Gold	Anti-EGFR	Squamous cell carcinoma	[136]
PF-HA-Cur@AuNPs	Curcumin	FITC & rhodamine B isothiocyanate	Anti-CD44 & folic acid	Cervical, colorectal, brain cancer	[137]
Silver + Chitosan	Photothermal therapy (800 nm NIR)			Lung cancer	[139]
Silver	Silver	Silver		Lung, breast cancer & melanoma	[144]
Silver	Silver & paracetamol prodrug	Silver	Folic acid	Cervical cancer	[145]
Zinc oxide		Zinc + 64Cu	TRC105	Breast cancer	[150]
Iron oxide-zinc oxide Core-shell	Carcinoembryonic antigen	iron oxide-zinc oxide		Dendritic cell-based immunotherapy	[164]
FA-PEG-SS-PEI-SPIONs	PD-L1 – siRNA	SPIONs	Folate	Gastric cancer	[167]
Amylose & SPIONs	Survivin-siRNA	SPIONs	Folate	Liver cancer	[168]
AU NS	Photothermal therapy & VEGF-siRNA	Gold		Cancer cells overexpressing $\alpha_v\beta_3$ integrin	[169]

TABLE 3

Some illustrative toxicological studies of polymer and metal nanoparticles in vivo

Nanoparticle	Model	Toxicity symptoms	Reference
PEG-modified ovalbumin + Freund's complete adjuvant (FCA)	<ul style="list-style-type: none"> - Rabbit - Subcutaneous 	<ul style="list-style-type: none"> - Anti-PEG response in the majority of immunized animals. - PEG was not immunogenic when given with FCA till 100000 Mw. - Without FCA, animals didn't show anti-PEG antibody. 	[178]
PEG-PLA	<ul style="list-style-type: none"> - Female rats. - Intraperitoneal for 3 successive days starting from the 4th postnatal day. - 20 mg/kg & 40 mg/kg 	<ul style="list-style-type: none"> - The infantile stage: Small & high dose elevated catalase & superoxide dismutase (SOD) & glutathione peroxidase (GPx). High dose lowered Trolox equivalent antioxidant capacity (TEAC). - The adult stage: Small dose reduced protein carbonyl levels. Small & High dose reduced SOD and glutathione peroxidase (GPx). 	[189]
Iron oxide NPs + dimercaptosuccinic acid (DMSA)	<ul style="list-style-type: none"> - Pregnant mice - Intraperitoneal - 3-9 nm - 50 mg/kg 	<ul style="list-style-type: none"> - No change in the number & weight of pups. - Significant growth inhibition. - Male infants; a significant decrease in the number of spermatogonia, spermatocytes, spermatids and mature sperm. - The NPs were present in the fetal liver & placenta. 	[190]
Iron oxide NPs	<ul style="list-style-type: none"> - Zebrafish - 30 nm original size but 1.025 µm after aggregation - 10 mg/L 	<ul style="list-style-type: none"> - Increase in the mortality rate. - Embryonic malformation. - Delayed hatchability. 	[191]
Iron oxide NPs	<ul style="list-style-type: none"> - Rat - Intra-tracheal installation - 22 & 280 nm - 0.8 & 20 mg/kg - Acute & chronic administration 	<ul style="list-style-type: none"> - Lung oxidative stress. - Trapping of the NPs by alveolar macrophage & lung epithelium. - Overloading of alveolar macrophage occurred with high doses. - Chronic administration with high dose causes lung emphysema, lung fibrosis. - Several inflammatory responses such as inflammatory and immune cells infiltration. - Clinical, pathological changes such as lymph node follicular hyperplasia, protein effusion, pulmonary vessel hyperemia and alveolar lipoproteinosis. - Longer coagulation time was detected with 22 nm low dose. 	[192]
Silver NPs	<ul style="list-style-type: none"> - Rat - Inhalation - 18 nm - low dose: 0.7 × 10(6)NPs/cm³ - Middle dose: 1.4 × 10(6)NPs/cm³ - High dose: 2.9 × 10(6)NPs/cm³ 6 h/day for 90 days. 	<ul style="list-style-type: none"> - Increase the inflammatory response associated with high dose. - Dose-dependent lesions such as chronic alveolar inflammation, thickness of alveolar walls and small granulomatous lesions. - Lung function affection: significant decrease of the tidal volume and minute volume. 	[193]
Gold NPs	<ul style="list-style-type: none"> - Rat - Intraperitoneal - 20 nm - 20 µg/kg for 3 successive days. 	<ul style="list-style-type: none"> - Generation of oxidative stress in rat brain by: Inhibition of antioxidant enzyme glutathione peroxidase. - Potentiate DNA damage and cell death by: Stimulation of 8-hydroxyguanosine, caspase-3 & heat shock protein 70. - Potentiate behavior disturbance by: Decrease the level of neurotransmitter dopamine and serotonin. Potentiate inflammation by increasing INF-γ 	[194]
Zinc oxide NPs	<ul style="list-style-type: none"> - Rat - Intraperitoneal for 10 days - 10-30 nm 	<ul style="list-style-type: none"> - Change in liver enzyme: A significant increase of aspartate aminotransferase (AST) in all groups but significant increase in alanine aminotransferase (ALT) only in 150 & 200 mg/kg. 	[195]

Nanoparticle	Model	Toxicity symptoms	Reference
	- 50, 100, 150 and 200 mg/kg	<ul style="list-style-type: none"> - Sperm: All the doses cause change in sperm morphology& decrease sperm count and vitality. Impairment of sperm motility was dose-dependent. - Liver histology was changed with doses higher than 50 mg/kg such as: Kupffer cells, congestion and chromatin condensation - Kidney histology was changed with doses above 50 mg/kg such as: Increase number of glomerular cells, congestion, and inflammation 	